Available online at www.sciencedirect.com
SCIENCE DIRECT®
ELSEVIER
International Journal of Solids and Structures 43 (2006) 3542–3568
INTERNATIONAL JOURNAL OF SOLIDS and STRUCTURES
www.elsevier.com/locate/ijsolstr

A stochastic constitutive model for disordered cellular materials: Finite-strain uni-axial compression

M.W. Schraad *, F.H. Harlow

Fluid Dynamics Group, Theoretical Division, Los Alamos National Laboratory, Mail Stop B216, Los Alamos, NM 87545, United States

Received 1 March 2005; received in revised form 18 May 2005
Available online 11 July 2005

Abstract

A stochastic constitutive model is developed for describing the continuum-scale mechanical response of disordered cellular materials. In the present work, attention is restricted to finite-strain uni-axial compression under quasi-static loading conditions. The development begins with an established cellular-scale mechanical model, but departs from traditional modeling approaches by generalizing the cellular-scale model to accommodate finite strain. The continuum-scale model is obtained by averaging the cellular-scale mechanical response over an ensemble of foam cells. Various stochastic material representations are considered through the use of probability density functions for the relevant material parameters, and the effects of the various representations on the continuum-scale response are investigated. Combining cellular-scale mechanics with a stochastic material representation to derive a continuum-scale constitutive model offers a promising new approach for simulating the finite-strain response of cellular materials. Results demonstrate that increasing a material's degree of polydispersity can produce the same stiffening effects as increasing the initial solid-volume fraction. Additionally, particular stochastic material representations are shown to provide upper and lower bounds on the mechanical response of the cellular materials under investigation, while suitable choices for the stochastic representation are shown to accurately reproduce experimental stress–strain data through the large deformations associated with densification.
Published by Elsevier Ltd.

Keywords: Microstructures; Constitutive behavior; Finite strain; Foam material; Probability and statistics

1. Introduction

Cellular materials are used extensively in a variety of applications. The most widely used cellular materials are natural cellular solids, such as wood and sponge, but polymers and metals have been the

* Corresponding author. Tel.: +1 505 665 3946; fax: +1 505 665 5926.
E-mail address: schraad@lanl.gov (M.W. Schraad).

0020-7683/$ - see front matter Published by Elsevier Ltd.
doi:10.1016/j.ijsolstr.2005.05.018

traditional materials selected for the synthesis and manufacture of foams and honeycombs, and ceramics are becoming the material of choice for many engineering purposes. Cellular materials are used in water and air filtration systems, for thermal and sound insulation, and in many structural applications. Structural foams, furthermore, can be soft and flexible, such as the packaging material and stress pads used for load and shock mitigation, or they can be stiff, but still deformable, such as those employed in energy absorption applications or those used as cores for sandwich structures. In the present work, attention is restricted to the class of flexible cellular solids with disordered structure that are used for cushioning, padding, and packaging materials. Of specific interest are polymeric foams, for which the primary objective is the development of a continuum-scale constitutive model for simulating finite-strain uni-axial compression.

Many issues conspire to make the development of a physically based constitutive model for cellular materials a substantial challenge. The properties and highly nonlinear mechanical response exhibited by cellular materials at the continuum scale are directly related to the mechanisms of deformation occurring in the structure found at the level of an individual foam cell. At the cellular scale, the structure is comprised of an intricate, interconnected network of cells. Cell edges are defined by relatively slender struts and cell faces, if closed, by thin films. Under compressive loading conditions, bending and stretching of the struts and films are the dominant deformation mechanisms. Nonlinear effects associated with finite strains, coupled with a changing cellular geometry, and competing with the effects of cell-wall contact, lead to the characteristic physical behavior exhibited at the continuum scale. A model that spans the two length scales, therefore, is required.

The inherent relationship between the cellular structure and the macroscopic response dictates that any modeling effort begin with a cellular-scale mechanical response description. The disordered nature of the cellular structure, however, points to the usefulness of a stochastic material representation in the development of any continuum-scale constitutive model. Furthermore, the large deformations these materials experience often are accompanied by fully three-dimensional stress and strain states, the evolving cellular geometry and the friction associated with cell-wall contact leads to prevalent strain-path dependence, and the visco-elastic nature of the parent solid leads to rate-dependent behavior. The porous nature of the cellular structure only complicates matters, as the evolving pressures and flow behavior of the permeating fluid affect the stiffness and rate-dependent response of these material systems. Each of these issues can be addressed, however, and previous researchers have done much to provide an excellent starting point.

Synthetic cellular materials first appeared in the late 1930s in the form of latex rubber foams. Talalay (1949) possibly was the first to note that the relative density, or solid-volume fraction, of a cellular material is the single most important material parameter for use in determining the corresponding macroscopic properties of cellular solids and the first to experimentally study the effects of cell size and shape on the continuum-scale response of these materials.

The mechanical behavior of these unique materials was not studied in detail until some time later. Among the earliest investigations into the mechanics of cellular materials are the works of Gent and Thomas (1959a,b, 1963). These early theoretical investigations represent the first attempts to relate the continuum-scale response of cellular materials to the physical mechanisms of deformation occurring at the cellular scale and the first to use an idealized cell-level model for such purposes. Similar attempts to model the macroscopic response of these materials followed, but these earliest investigators understood that their models were idealized representations of actual cellular solids and that, in reality, the cellular materials they studied were far from homogeneous, with a variety of cell shapes, orientations, and sizes. A review of early contributions in this area is provided by Hilyard (1982).

Subsequent attempts to model the macroscopic response of cellular materials generally fall into one of two categories. The first category includes other cellular-scale mechanical models, like those of Gent and Thomas, which are based on the simplified mechanics of a single, idealized, foam cell or suitable representative structure. Gibson, Ashby, and their co-workers (see Gibson et al., 1982; Gibson and Ashby, 1982; Ashby, 1983) devoted themselves to understanding cell-level structural mechanics and relating the

deformation mechanisms at this scale to the continuum-scale response of honeycombs and foams. Indeed, the most often referenced work in the fields of cellular material mechanics and modeling is the now classic text of Gibson and Ashby (1988). In each of these works, the nonlinear compressive behavior of cellular materials is simplified to a tri-linear response broken down into an initial linearly elastic regime, a constant-stress load plateau, and a stiff densification regime. The macroscopic properties of cellular materials in each regime of compressive behavior, as well as in tension and shear, are correlated to a specific mechanism of deformation occurring in the single-cell model when subjected to the appropriate corresponding loading condition.

Other cell-level modeling efforts followed, but remained based on the mechanics of perfectly ordered structures. While Gibson and Ashby focused on an idealized foam cell, Warren and Kraynik (1987, 1988, 1991, 1997) and Warren et al. (1989) focused on an even smaller representative structure—an idealized cell vertex—in their investigations into the properties and behavior of these materials. More recently, Zhu et al. (1997) used a representative substructure of a body-centered-cubic lattice of tetrakaidecahedral cells to analyze the high-strain response of foams. Their work appears to be unique, in that they compare their quasi-single-cell results to experimental data obtained for a single foam cell.

The single-cell view, while illustrative, assumes a uniformity in the underlying cellular structure that is not present, and thus, can lead to gross over or under predictions of stress levels for given levels of strain. Additionally, most often, the single-cell approach has been used to calculate initial linearly elastic properties of cellular materials, but rarely to generate a description of the evolving nonlinear properties or to construct a fully three-dimensional constitutive model that is valid for large deformations.

The second category of cellular material models includes those that are derived from detailed numerical simulations; for example, those involving finite-element discretizations of real, or at least realistic, cellular structures containing a statistically meaningful number of foam cells. Direct numerical simulations of such representative structures then can be carried out to determine the macroscopic response of the materials comprised of such structures. Kraynik et al. (1999) used finite-element analysis to study the mechanical response of perfectly ordered, three-dimensional, open- and closed-cell foams to uni-axial and hydrostatic compression. Zhu et al. (2000) and Zhu and Windle (2002) used finite-element analysis to investigate the effects of cell irregularity on the initial properties and the high-strain compression of open-cell foams. And as an extension of the work of Triantafyllidis and Schraad (1998) for two-dimensional honeycombs, Laroussi et al. (2002) used numerical simulations to explore the nonlinear response of materials with three-dimensional, periodic, cellular micro-structures.

When formulated properly, the results of a detailed numerical study can be as illuminating as well-conducted experiments. An obvious and significant advantage of using a numerical technique to study cellular materials is that it permits a detailed representation of the cellular geometry and the material properties of the parent solid. Unfortunately, numerical analyses—especially finite-element methods—often succumb to problems associated with large deformations and contact long before reaching the finite strains for which these materials are intended. Also, because the materials of interest exhibit highly nonlinear behavior, their mechanical properties depend strongly on both strain and strain history, and thus, these numerical techniques cannot be used in the construction of a constitutive model—except in the same guiding capacity as good experimental data.

In the present work, attention is restricted to the development of a constitutive model for simulating the continuum-scale mechanical response of disordered cellular materials to finite-strain uni-axial compression under quasi-static loading conditions. Modeling the three-dimensional, rate-dependent, dynamic response of such materials requires a tensorial form for the constitutive model, a proper accounting of frictional and visco-elastic effects, and a description of the coupled effects of the permeating fluid. Extensions of the constitutive model developed here for such situations are the subjects of several forthcoming articles.

The constitutive model development begins with a cellular-scale mechanical response description generalized to accommodate finite strain. As in previous studies, the mechanical model used is based on cellular-

scale deformation mechanisms. But unlike in previous studies, the nonlinear response associated with large deformations is considered. The cellular-scale mechanical model then is averaged over an ensemble of foam cells, forming a continuum-scale constitutive model that relates the macroscopic stress rate in the cellular material to the macroscopic strain rate. Various stochastic representations then are considered through the use of probability density functions for the relevant material parameters, and closures for the continuum-scale model are obtained.

The stochastic constitutive model is used to calculate the continuum-scale mechanical response of a low-density, open-cell, polyurethane foam. The response obtained using the stochastic model is compared to experimental stress–strain data for finite-strain uni-axial compression, and the effects of various stochastic material representations on the macroscopic behavior are investigated. Results demonstrate that increasing a material's degree of polydispersity can produce the same stiffening effects as increasing the initial solid-volume fraction. Additionally, particular stochastic representations are shown to provide upper and lower bounds on the stress–strain response of the cellular material under investigation, while suitable choices for the stochastic representation are shown to accurately reproduce the stress–strain response through the large deformations associated with densification, where most other models and direct numerical simulations fail.

2. Cellular-scale constitutive model

Consider a low-density, open-cell, polyurethane foam, such as the sample shown in Fig. 1. Traditional approaches for modeling the mechanical response of such materials are reviewed in Section 1. These approaches typically focus on the development of expressions for the initial material properties in terms of the cellular-scale geometry, the properties of the parent solid, and the relative density, or solid-volume fraction, of the material. In this section, the development of the continuum-scale constitutive model begins with just such an expression for the initial tangent modulus of the material. The nonlinear response associated with large deformations, however, also is considered, and the cellular-scale mechanical model is generalized to accommodate finite strain.

Gibson and Ashby (1988) show that, for a broad class of disordered cellular materials, the initial Poisson's ratio, $\nu_0^{\mathrm{c}} \approx 1/3$. Zhu et al. (2000) and Zhu and Windle (2002), however, show that Poisson's ratio decreases rapidly with increasing compressive strain and that for low-density open-cell foams, the finite-strain Poisson's ratio can be as small as 0.02. In the derivation to follow, therefore, Poisson's ratio is approximated as zero, and no distinction is made between uni-axial stress and uni-axial strain. Under such circumstances, the initial tangent modulus for a cellular material, denoted here by E_0^{c}, is defined as

$$E_0^{\mathrm{c}} \equiv \left.\frac{\mathrm{d}\sigma}{\mathrm{d}\epsilon}\right|_{\epsilon=0}, \tag{1}$$

in which σ is the continuum-scale stress and ϵ the continuum-scale strain. Gibson and Ashby (1988), Warren and Kraynik (1988), Van Der Burg et al. (1997), and many others, show that for an open-cell foam, the initial tangent modulus can be written as

$$E_0^{\mathrm{c}} = A_0 E^{\mathrm{s}} \phi_0^2, \tag{2}$$

in which the parameter, A_0, is a geometric constant of proportionality, E^{s} is the tangent modulus of the parent solid (assumed to be constant), and ϕ_0 is the initial solid-volume fraction of the material. Here, the subscripts are used to denote initial material properties, which are relevant only for infinitesimal strain.

Despite being applied at the continuum scale, the relationship provided in Eq. (2) is derived by considering the mechanics of a single, idealized, foam cell or suitable representative structure and by assuming that cell-wall bending is the dominant mechanism of deformation occurring at the cellular scale. Analysis of any particular open-cell geometry under compressive loading conditions leads to this relationship.

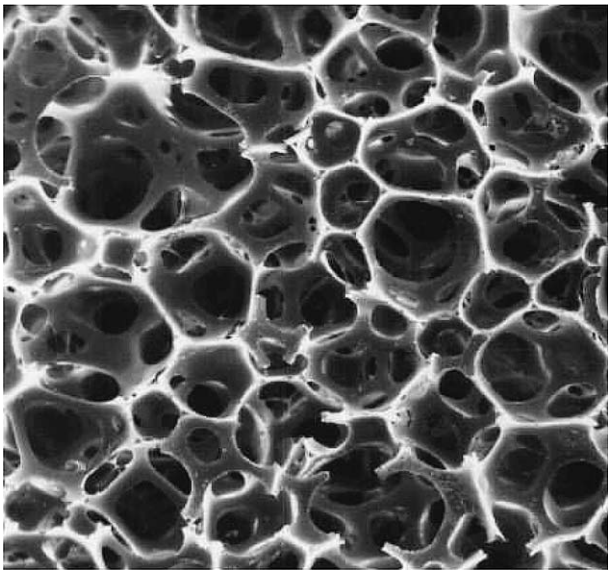

Fig. 1. A scanning electron micrograph of a low-density, open-cell, polyurethane foam showing the intricate structure at the cellular scale. This material was provided courtesy of the Dow Chemical Company, and the micrograph was provided courtesy of Dr. D.J. Alexander of the Materials Science & Technology Division (MST-6) at Los Alamos National Laboratory. The continuum-scale response of this material is inherently related to the cellular-scale geometry, the properties of the parent solid, and the relative density, or solid-volume fraction, of the material. Bending in the struts is the dominant deformation mechanism at the cellular scale when such a material is subjected to uni-axial compression.

Different cell geometries lead to different values of the parameter, A_0, as do different orientations of a particular cell to the direction of loading, different strut geometries, or different constraints at the cell vertices.

Because cellular materials retain their cellular structure through all deformations up to full densification, and because cell-wall bending remains the dominant mode of deformation at the cellular scale for low-density open-cell foams subjected to compressive deformations, it is postulated that the tangent modulus maintains the functional form presented in Eq. (2) through all deformations as well. When subjected to compression, however, the cellular-scale geometry and solid-volume fraction evolve with strain. In other words, the geometric "constant" of proportionality, A (henceforth, referred to as the geometric stiffness), and the solid-volume fraction, ϕ, are functions of strain, and thus, the tangent modulus, E^{c}, is a function of strain as well. That is

$$E^{\mathrm{c}}(\epsilon) = A(\epsilon)E^{\mathrm{s}}[\phi(\epsilon)]^2, \tag{3}$$

in which $A(0) = A_0$, $\phi(0) = \phi_0$, and $E^{\mathrm{c}}(0) = E^{\mathrm{c}}_0$.

The relative density, or solid-volume fraction, of a particular foam cell is defined as the ratio of the density associated with the foam cell, ρ^{c}, to the density of the parent solid, ρ^{s}. That is

$$\phi \equiv \frac{\rho^{\mathrm{c}}}{\rho^{\mathrm{s}}} = \frac{m^{\mathrm{c}}}{V^{\mathrm{c}}}\frac{V^{\mathrm{s}}}{m^{\mathrm{s}}}, \tag{4}$$

in which m^{c} and V^{c} are the mass and volume associated with the foam cell, and m^{s} and V^{s} are the mass and volume of the solid material comprising the cellular structure. But the mass associated with the foam cell must equal the mass of the solid material comprising the cell. That is

$$m^{\mathrm{c}} = m^{\mathrm{s}}. \tag{5}$$

Also, because bulk polyurethane is nearly incompressible under quasi-static loading conditions, and because only a small fraction of solid material is expected to reach a finite level of strain (even for finite-strain compression of the cellular material), it can be assumed that

$$V^{s} \approx \text{constant}. \tag{6}$$

Furthermore, for uni-axial compression of a cellular material (assuming $v^{c} \approx 0$), it can be shown that

$$V^{c} = V_0^{c}(1+\epsilon) \tag{7}$$

in which V_0^{c} is the initial volume of the foam cell. Substitution of Eqs. (5) and (7) into Eq. (4) then provides

$$\phi(\epsilon) = \frac{V^{s}}{V_0^{c}(1+\epsilon)} = \frac{\phi_0}{1+\epsilon} \tag{8}$$

in which $\phi_0 = V^{s}/V_0^{c}$ is the initial solid-volume fraction of the particular foam cell under consideration.

The effects of an evolving cellular-scale geometry on the geometric stiffness, A, are more difficult to quantify. For a particular foam cell, the exact value of A depends on cell shape, orientation, strut geometry (e.g., strut cross-sectional shape and constraints at the cell vertices), and strain. Analysis of any realistic cellular geometry to determine all possible initial values of A, for all possible cell shapes, orientations, and strut geometries, likely presents an intractable task. Analysis of any realistic cellular geometry to account for the nonlinear effects associated with finite bending strains in the cell walls is virtually guaranteed to be impossible. Using the physical behavior at the cellular scale as a guide, however, a simple, yet useful, approximation can be made.

Cellular materials soften with increasing compressive deformations, as shown in Fig. 2. This decrease in stiffness is due to the increasing misalignment of material with the direction of loading that accompanies finite bending strains. The softening continues until the competing mechanism of cell-wall contact begins to dominate the response at moderate strain, and a gradual increase in stiffness is induced. This stiffening continues, and as the deforming structure approaches full densification, the tangent modulus of the cellular material approaches the tangent modulus of the parent solid.

With regard to the mechanical response of an individual foam cell, the geometric stiffness, A, decreases with increasing compressive deformations until cell-wall contact occurs. The value of A, however, is bounded from below at this point by the theoretical limit of zero, which corresponds to the buckling load of the cell for a particular initial configuration (see Gibson and Ashby, 1988). The geometric stiffness, however, never reaches this theoretical limit, because disordered cellular materials lack the symmetries necessary for such bifurcations to occur. After cell-wall contact, the geometric stiffness, A, remains constant through moderate strain. The continued increase in the cell stiffness in this regime of behavior is associated with the process of densification [i.e., $E^{c} \sim 1/(1+\epsilon)^2$]. As the material approaches full densification, however, the geometric stiffness once again increases, and the value of A is bounded from above at this point by $\lim_{\epsilon \to -1+\phi_0} E^{c} = E^{s}$.

An estimate of the average value of the geometric stiffness, A, for an ensemble of foam cells can be obtained at any value of strain by examining the slope of the stress–strain curve for the material of interest, as shown in Fig. 2. Therefore, as a first approximation to the response of an individual foam cell, consider the following tri-linear approximation to the function $A(\epsilon)$:

$$A(\epsilon) = A_0 H(\epsilon - \epsilon_1) + A_1 H(\epsilon_1 - \epsilon) + (A_2 - A_1) H(\epsilon_2 - \epsilon). \tag{9}$$

Here, ϵ_1 and ϵ_2 are transition strains corresponding to the onset of softening and to full densification, respectively, in the foam cell; A_0, A_1, and A_2 are the values of the geometric stiffness evaluated at $\epsilon = 0$, $\epsilon = \epsilon_1$, and $\epsilon = \epsilon_2$, respectively; and the function, $H(x)$, is the Heaviside step function, defined by

$$H(x) = \begin{cases} 1, & x \geqslant 0 \\ 0, & x < 0. \end{cases} \tag{10}$$

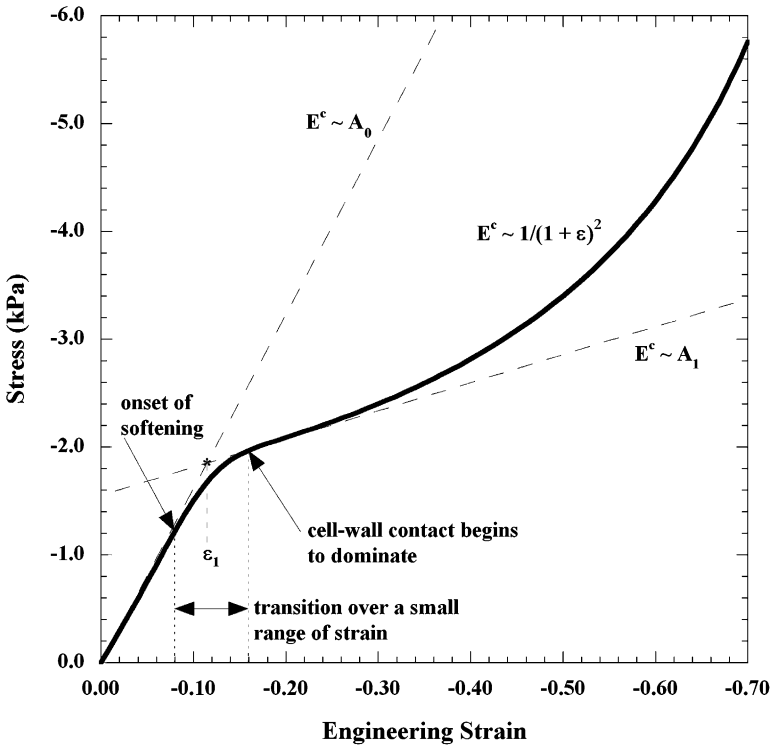

Fig. 2. The continuum-scale stress–strain response of a cellular material subjected to quasi-static uni-axial compression. Characteristic features and mechanism-dependent behavior are identified. The analagous components of the cellular-scale mechanical model also are shown for purposes of comparison.

Substituting the relations provided in Eqs. (8) and (9) into Eq. (3) results in the following expression for the tangent modulus of the foam cell:

$$E^{c}(\epsilon) = \frac{[A_0 H(\epsilon - \epsilon_1) + A_1 H(\epsilon_1 - \epsilon) + (A_2 - A_1) H(\epsilon_2 - \epsilon)] E^{s} \phi_0^2}{(1+\epsilon)^2}. \tag{11}$$

A foam cell reaches full densification (i.e., $E^{c} \equiv E^{s}$), however, for $\epsilon \approx -1 + \phi_0$, and it follows from Eq. (11) that:

$$E^{c}(-1+\phi_0) = (A_1 + A_2 - A_1) E^{s} \frac{\phi_0^2}{(1-1+\phi_0)^2} = A_2 E^{s} \approx E^{s}, \tag{12}$$

which suggests either

$$A_2 \approx 1 \quad \text{for } \epsilon_2 = -1 + \phi_0 \tag{13}$$

or

$$A_2 = 1 \quad \text{for } \epsilon_2 \approx -1 + \phi_0. \tag{14}$$

By employing the latter, the tri-linear approximation to the function, $A(\epsilon)$, can be rewritten as

$$A(\epsilon) = A_0 H(\epsilon - \epsilon_1) + A_1 H(\epsilon_1 - \epsilon) + (1 - A_1) H(\epsilon_2 - \epsilon) \tag{15}$$

and the tangent modulus for the foam cell becomes

$$E^{c}(\epsilon) = \frac{[A_0 H(\epsilon - \epsilon_1) + A_1 H(\epsilon_1 - \epsilon) + (1 - A_1) H(\epsilon_2 - \epsilon)] E^{s} \phi_0^2}{(1+\epsilon)^2}. \tag{16}$$

In this way, the rate form of the constitutive model at the cellular scale can be written as

$$\dot{\sigma} = E^{c}(\epsilon)\dot{\epsilon} \tag{17}$$

in which $\dot{\sigma}$ and $\dot{\epsilon}$ are the rates of stress and strain, respectively, for an individual foam cell.

Of course, the tri-linear form of the constitutive model is an approximation to the actual mechanical response of an individual foam cell. This approximation, however, can be used to model all uni-axial compressive deformations of the cell up to full densification of the material and beyond (i.e., for $\epsilon \to -1$).

Most previous modeling efforts apply the relationship provided in Eq. (2) directly to the continuum scale. This is, however, only useful for describing how an individual foam cell responds to infinitesimal compressive strain. To obtain the continuum-scale response to large deformations for a cellular material comprised of a collection of many cells, one must average the finite-strain response of the individual foam cell over the entire ensemble, allowing for stochastic variations in the material parameters. In this way, the discontinuities associated with the tri-linear approximation for an individual cell are smoothed through the averaging process. This averaging process, and the resulting continuum-scale constitutive model, are outlined in Section 3.

3. Continuum-scale constitutive model

Previous researchers have firmly established the relationship among the initial continuum-scale mechanical properties of cellular materials, the intricate structure found at the level of an individual foam cell, the properties of the parent solid, and the relative density, or solid-volume fraction. Most often, this relationship is expressed as an equation for the initial tangent modulus of the material. In Section 2, an established cellular-scale mechanical model is introduced and extended to accommodate finite strain by considering the effects of a changing cellular geometry and an evolving material density. In this section, the continuum-scale constitutive model is obtained by taking appropriate averages of the cellular-scale model over an ensemble of many foam cells.

The rate form of the constitutive model for an individual foam cell is given by Eq. (17), and the corresponding strain-dependent tangent modulus is given by Eq. (16). These equations provide a description of the mechanical response for any particular foam cell taken at random from a collection of foam cells comprising an ensemble of similar foam samples. To obtain a constitutive model at the continuum scale for such a material, this cellular-scale model must be averaged over the ensemble. That is,

$$\bar{\dot{\sigma}} = \overline{E^{c}(\epsilon)\dot{\epsilon}} = \overline{E^{c}(\epsilon)}\,\bar{\dot{\epsilon}} + \overline{E^{c\prime}(\epsilon)\dot{\epsilon}'}. \tag{18}$$

Here, a line over any quantity denotes that quantity's properly weighted ensemble average, so $\overline{E^{c}(\epsilon)}$ is the average tangent modulus of the cellular material, and $\bar{\dot{\sigma}}$ and $\bar{\dot{\epsilon}}$ are the average stress and strain rates, respectively. The quantities, $E^{c\prime}(\epsilon)$ and $\dot{\epsilon}'$, are fluctuations in the cellular-scale modulus and strain rate, respectively, and therefore, the term, $\overline{E^{c\prime}(\epsilon)\dot{\epsilon}'}$, represents an average of the cross correlation between these two quantities.

Terms such as $\overline{E^{c}(\epsilon)}$, $\bar{\dot{\epsilon}}$, etc., represent averages over many cells taken at random from an ensemble of similar foam samples. Ergodically, this is equivalent to averages over a volume of many cells taken from a single cellular material system. The ensemble-averaged quantities, therefore, are equivalent to volume-averaged, continuum-scale quantities. In this sense, these terms are synonomous, and are treated as such for the remainder of this discussion.

In general, the cross-correlation term, $\overline{E^{c\prime}(\epsilon)\dot{\epsilon}'}$, requires modeling, and often, direct numerical simulations to verify that the model fits empirical data. Schjødt-Thomsen and Pyrz (2004), however, use numerical techniques to show that strain fluctuations are small in three-dimensional random dispersions of cells subjected to various loading conditions, and they suggest the traditional approach offered by Voigt (1889) for modeling strain can lead to reasonably accurate approximations to the actual strain response of disordered cellular materials.

3.1. Voigt approximation

The Voigt approximation simplifies the form of the continuum-scale constitutive model by assuming the strain fluctuations are negligible. Therefore, consider

$$\epsilon' = 0 \Rightarrow \epsilon = \overline{\epsilon} \tag{19}$$

in which ϵ' is the strain fluctuation for the individual foam cell, ϵ is the cell strain, and $\overline{\epsilon}$ is the average strain for an ensemble of cells (i.e., $\epsilon = \overline{\epsilon} + \epsilon'$). Equivalently, one can assume

$$\dot{\epsilon}' = 0 \Rightarrow \dot{\epsilon} = \overline{\dot{\epsilon}}. \tag{20}$$

Eqs. (19) and (20) state that the strain, and thus the strain rate, are the same for all cells in the ensemble, and therefore, the local cellular-scale strain and strain-rate fields do not vary with position.

Because the strain-rate fluctuations are assumed to be zero, the cross-correlation term in Eq. (18) also is zero. The continuum-scale constitutive model then reduces to

$$\overline{\dot{\sigma}} = \overline{E^{c}(\overline{\epsilon})}\overline{\dot{\epsilon}} \tag{21}$$

and it remains to determine the average tangent modulus $\overline{E^{c}(\overline{\epsilon})}$.

3.2. Reuss approximation

Alternatively, the cellular-scale constitutive model can be rewritten as

$$\dot{\epsilon} = C^{c}(\epsilon)\dot{\sigma} \tag{22}$$

in which

$$C^{c}(\epsilon) = \frac{1}{E^{c}(\epsilon)} \tag{23}$$

is the cellular-scale compliance.

Averaging over an ensemble of foam cells provides

$$\overline{\dot{\epsilon}} = \overline{C^{c}(\epsilon)\dot{\sigma}} = \overline{C^{c}(\epsilon)}\overline{\dot{\sigma}} + \overline{C^{c\prime}(\epsilon)\dot{\sigma}'}. \tag{24}$$

Here, $\overline{C^{c}(\epsilon)}$ is the average compliance of the cellular material, the quantities $C^{c\prime}(\epsilon)$ and $\dot{\sigma}'$ are fluctuations in the cellular-scale compliance and stress rate, respectively, and the term, $\overline{C^{c\prime}(\epsilon)\dot{\sigma}'}$, represents an average of the cross correlation between these two quantities.

Again, in general, the cross-correlation term, $\overline{C^{c\prime}(\epsilon)\dot{\sigma}'}$, requires modeling, however, similar to the approach taken above, one can assume that the traditional approach offered by Reuss (1929) for modeling stress will lead to reasonably accurate approximations to the actual stress response of disordered cellular materials.

The Reuss approximation also simplifies the form of the continuum-scale constitutive model by assuming the stress fluctuations are negligible. Therefore, consider

$$\sigma' = 0 \Rightarrow \sigma = \overline{\sigma}, \tag{25}$$

in which σ' is the stress fluctuation for the individual foam cell, σ is the cell stress, and $\overline{\sigma}$ is the average stress for an ensemble of cells (i.e., $\sigma = \overline{\sigma} + \sigma'$). Equivalently, one can assume

$$\dot{\sigma}' = 0 \Rightarrow \dot{\sigma} = \overline{\dot{\sigma}}. \tag{26}$$

Eqs. (25) and (26) state that the stress, and thus the stress rate, are the same for all cells in the ensemble, and therefore, the local cellular-scale stress and stress-rate fields do not vary with position.

Because the stress-rate fluctuations are assumed to be zero, the cross-correlation term in Eq. (24) also is zero. The continuum-scale constitutive model then reduces to

$$\overline{\dot{\epsilon}} = \overline{C^{c}(\epsilon)\dot{\sigma}} \tag{27}$$

and it remains to determine the average compliance, $\overline{C^{c}(\epsilon)}$.

Dealing with this particular form of the continuum-scale constitutive model, however, presents some difficulties, because the cellular-scale compliance is constructed as a function of strain, and so, the average compliance remains a function of strain as well. To evaluate the average compliance, the rate form of the cellular-scale constitutive model must be integrated and the resulting stress–strain model must be inverted before the Reuss approximation can be used. While nontrivial, this can be done in principle, provided the stress is a monotonically increasing function of strain. In other words, one must determine $\epsilon = f(\sigma) = f(\overline{\sigma})$ and substitute this relation into Eq. (27) to obtain

$$\overline{\dot{\epsilon}} = \overline{C^{c}(f(\overline{\sigma}))\dot{\sigma}}. \tag{28}$$

This relation then can be inverted to obtain the continuum-scale constitutive model in the usual rate form.

To limit the scope of the present work, attention is restricted to the use of the Voigt approximation for the remainder of this discussion. In the next section, various stochastic material representations are considered through the use of probability density functions for the relevant material parameters. The various stochastic representations are used to determine corresponding expressions for the average tangent modulus of the cellular material. By substituting these expressions into Eq. (21), the resulting continuum-scale stress–strain response can be obtained.

4. Stochastic material representation

In Section 2, a nonlinear constitutive model is developed to describe the mechanical response of an individual foam cell to finite-strain uni-axial compression. In Section 3, this cellular-scale constitutive model is averaged over an ensemble of foam cells, forming a continuum-scale description of the mechanical response for a cellular material. It remains to determine the average tangent modulus of the cellular material, which depends on cell-to-cell fluctuations in the parameters that describe the individual foam cell response. In this section, various stochastic material representations are examined and used to obtain the corresponding continuum-scale constitutive model in closed form.

At the cellular scale, the tangent modulus for an individual foam cell is given by Eq. (16). In general, it is expected that all of the material parameters, A_0, A_1, ϵ_1, ϵ_2, E^{s}, and ϕ_0, along with the individual cell strain, ϵ, vary from cell to cell in an ensemble of foam cells, when random samples of the cellular material are subjected to any macroscopic loading. Therefore, all of the material parameters, along with the individual cell strain, are treated as independent variables in the stochastic material representation, and in general, the average tangent modulus is given by

$$\overline{E^{c}} \equiv \int_{A_0}\int_{A_1}\int_{\epsilon_1}\int_{\epsilon_2}\int_{E^{s}}\int_{\phi_0}\int_{\epsilon} E^{c}(\epsilon)P\,\mathrm{d}\epsilon\,\mathrm{d}\phi_0\,\mathrm{d}E^{s}\mathrm{d}\epsilon_2\,\mathrm{d}\epsilon_1\,\mathrm{d}A_1\,\mathrm{d}A_0, \tag{29}$$

in which $E^{c}(\epsilon)$ is the tangent modulus of any particular foam cell in an ensemble of cells, and the quantity $P\,\mathrm{d}\epsilon\,\mathrm{d}\phi_0\,\mathrm{d}E^{s}\,\mathrm{d}\epsilon_2\,\mathrm{d}\epsilon_1\,\mathrm{d}A_1\,\mathrm{d}A_0$ is the probability that this particular foam cell is characterized by the parameters, A_0, in the interval $\mathrm{d}A_0$; A_1, in the interval $\mathrm{d}A_1$; …; ϕ_0, in the interval $\mathrm{d}\phi_0$; and by the strain, ϵ, in the interval $\mathrm{d}\epsilon$. The function P is the probability density function.

4.1. Uncorrelated variables

The cellular-scale constitutive model is derived in such a way that the effects of the cellular-scale geometry, the properties of the parent solid, and the solid-volume fraction on the tangent modulus of the individual foam cell are uncorrelated. Therefore, consider the case for which all of the independent variables in the stochastic material representation are uncorrelated. In this case, the probability density function assumes the following form:

$$P = P_{A_0}(A_0)P_{A_1}(A_1)P_{\epsilon_1}(\epsilon_1)P_{\epsilon_2}(\epsilon_2)P_{E^{s}}(E^{s})P_{\phi_0}(\phi_0)P_{\epsilon}(\epsilon) \tag{30}$$

in which $P_{A_0},\ P_{A_1},\ldots,P_{\epsilon}$ are the probability density functions associated with each of the respective uncorrelated independent variables.

By invoking the Voigt approximation, however, it is assumed that $\epsilon = \overline{\epsilon}$, and therefore

$$P_{\epsilon}(\epsilon) = \delta(\epsilon - \overline{\epsilon}) \tag{31}$$

in which the function, $\delta(x)$, is the Dirac delta function, defined by

$$\int_{x_1}^{x_2} f(x)\delta(x)\mathrm{d}x = \begin{cases} 1, & x_1 < x < x_2, \\ 0, & \text{otherwise.} \end{cases} \tag{32}$$

Substitution of the relationship given in Eq. (31) into the probability density function expressed in Eq. (30), and subsequent substitution of the result into Eq. (29) provides the average tangent modulus for uncorrelated variables, which can be written as

$$\overline{E^{c}(\overline{\epsilon})} = \tilde{A}(\overline{\epsilon})\overline{E}^{s}[\tilde{\phi}(\overline{\epsilon})]^2 \tag{33}$$

in which the effective geometric stiffness is defined by

$$\tilde{A}(\overline{\epsilon}) \equiv \overline{A}_0 \int_{\epsilon_1} H(\overline{\epsilon} - \epsilon_1)P_{\epsilon_1}(\epsilon_1)\mathrm{d}\epsilon_1 + \overline{A}_1 \int_{\epsilon_1} H(\epsilon_1 - \overline{\epsilon})P_{\epsilon_1}(\epsilon_1)\mathrm{d}\epsilon_1 + (1 - \overline{A}_1)\int_{\epsilon_2} H(\epsilon_2 - \overline{\epsilon})P_{\epsilon_2}(\epsilon_2)\mathrm{d}\epsilon_2 \tag{34}$$

and the effective solid-volume fraction is defined by

$$\tilde{\phi}(\overline{\epsilon}) \equiv \left[\frac{1}{(1+\overline{\epsilon})^2}\int_{\phi_0} \phi_0^2 P_{\phi_0}(\phi_0)\mathrm{d}\phi_0\right]^{\frac{1}{2}}. \tag{35}$$

The expressions for the effective geometric stiffness and the effective solid-volume fraction depend on the average continuum-scale strain, $\overline{\epsilon}$, as well as on the probability density functions for the transition strains, ϵ_1 and ϵ_2, and the initial solid-volume fraction, ϕ_0. Therefore, the average tangent modulus evolves with strain and depends on the stochastic material representation as well.

Here, it is noted that the mean of any random variable, x, is defined as

$$\overline{x} \equiv \int_{-\infty}^{\infty} xP(x)\mathrm{d}x \tag{36}$$

and that the corresponding probability density function must satisfy the following relation:

$$\int_{-\infty}^{\infty} P(x)\mathrm{d}x \equiv 1. \tag{37}$$

Therefore, because the tangent modulus for an individual foam cell depends linearly on the geometric stiffness parameters, A_0 and A_1, and the initial tangent modulus of the parent solid, E^s, and because these variables are uncorrelated, the average tangent modulus only depends on the average values, $\overline{A}_0$, $\overline{A}_1$, and $\overline{E}^s$, rather than on the distributions of A_0, A_1, and E^s. Consequently, the resulting expression for the average tangent modulus assumes a relatively simple form.

4.2. Monodisperse distributions

Consider an idealized cellular material, for which the parameters describing the cellular-scale mechanical response of any particular foam cell are characterized by monodisperse distributions. In other words, each material parameter is constant over the entire ensemble of foam cells. While not realistic, this example demonstrates the similarities and differences between the stochastic model and previous approaches for modeling the continuum-scale stress–strain response of cellular materials. In this case, the probability density functions for the transition strains and the initial solid-volume fraction are given, respectively, by

$$P_{\epsilon_1}(\epsilon_1) = \delta(\epsilon_1 - \overline{\epsilon}_1), \tag{38}$$

$$P_{\epsilon_2}(\epsilon_2) = \delta(\epsilon_2 - \overline{\epsilon}_2), \tag{39}$$

and

$$P_{\phi_0}(\phi_0) = \delta(\phi_0 - \overline{\phi}_0). \tag{40}$$

For a cellular material characterized by monodisperse distributions, the effective geometric stiffness then is given by

$$\tilde{A}(\overline{\epsilon}) = \overline{A}_0 H(\overline{\epsilon} - \overline{\epsilon}_1) + \overline{A}_1 H(\overline{\epsilon}_1 - \overline{\epsilon}) + (1 - \overline{A}_1) H(\overline{\epsilon}_2 - \overline{\epsilon}) \tag{41}$$

and the effective solid-volume fraction is given by

$$\tilde{\phi}(\overline{\epsilon}) = \frac{\overline{\phi}_0}{1 + \overline{\epsilon}}. \tag{42}$$

Substitution of the relations provided in Eqs. (41) and (42) into the relation for the average tangent modulus provided in Eq. (33) yields

$$\overline{E^c(\overline{\epsilon})} = \frac{[\overline{A}_0 H(\overline{\epsilon} - \overline{\epsilon}_1) + \overline{A}_1 H(\overline{\epsilon}_1 - \overline{\epsilon}) + (1 - \overline{A}_1) H(\overline{\epsilon}_2 - \overline{\epsilon})] \overline{E}^s \overline{\phi}_0^2}{(1 + \overline{\epsilon})^2}. \tag{43}$$

This is the simplest form of the average tangent modulus representing the collective mechanical response of an ensemble of foam cells. It is analagous to applying a single-cell mechanical model to the continuum scale by replacing single-cell model parameters with their continuum-scale averages, and thus, is equivalent to many previous single-cell modeling efforts. A discontinuity in the tangent modulus necessarily results from using monodisperse distributions, however, this discontinuity is smoothed through the averaging process for more realistic, polydisperse, stochastic material representations.

4.3. Random distributions

Next, consider a cellular material, for which the parameters describing the cellular-scale mechanical response of any particular foam cell are characterized by random distributions. In other words, there exists an equal likelihood that a parameter, say A_0, takes on any particular value within some range of permissible

values. Because disordered cellular materials are not necessarily strictly random, this is an approximation. In this case, the probability density functions for the transition strains are given by

$$P_{\epsilon_1}(\epsilon_1) = \begin{cases} \dfrac{1}{2\Delta_{\epsilon_1}}, & \bar{\epsilon}_1 - \Delta_{\epsilon_1} \leqslant \epsilon_1 \leqslant \bar{\epsilon}_1 + \Delta_{\epsilon_1} \\ 0, & \text{otherwise} \end{cases} \tag{44}$$

and

$$P_{\epsilon_2}(\epsilon_2) = \begin{cases} \dfrac{1}{2\Delta_{\epsilon_2}}, & \bar{\epsilon}_2 - \Delta_{\epsilon_2} \leqslant \epsilon_2 \leqslant \bar{\epsilon}_2 + \Delta_{\epsilon_2} \\ 0, & \text{otherwise} \end{cases} \tag{45}$$

in which $2\Delta_{\epsilon_1}$ and $2\Delta_{\epsilon_2}$ are the ranges of permissible values of the transition strains, ϵ_1 and ϵ_2, respectively. The quantities, Δ_{ϵ_1} and Δ_{ϵ_2}, must be greater than zero, but must not be so large that the distributions become physically meaningless. For example, $-1 \leqslant \epsilon_1 \leqslant 0$ and $-1 \leqslant \epsilon_2 \leqslant 0$, and thus $\bar{\epsilon}_1 + \Delta_{\epsilon_1} \leqslant 0$ and $\bar{\epsilon}_2 - \Delta_{\epsilon_2} \geqslant -1$. Also, in general, a regime of deformation exists between the onset of softening and densification (the term "load plateau" is often applied to the corresponding portion of the stress–strain curve). This regime spans a finite range of strain, which is especially prolonged for highly ordered cellular materials. Therefore, it is reasonable to assume that $\bar{\epsilon}_2 + \Delta_{\epsilon_2} \leqslant \bar{\epsilon}_1 - \Delta_{\epsilon_1}$. These constraints ensure that the transition strains are physically realizable and provide lower and upper bounds on the permissible values of the transition strains for a particular foam cell.

Upon substitution of the relations provided in Eqs. (44) and (45), the integrals in Eq. (34) are evaluated as

$$\begin{aligned} \int_{\epsilon_1} H(\bar{\epsilon} - \epsilon_1) P_{\epsilon_1}(\epsilon_1) \mathrm{d}\epsilon_1 &= \int_{\bar{\epsilon}_1 - \Delta_{\epsilon_1}}^{\bar{\epsilon}_1 + \Delta_{\epsilon_1}} \frac{H(\bar{\epsilon} - \epsilon_1)}{2\Delta_{\epsilon_1}} \mathrm{d}\epsilon_1 = \frac{1}{2\Delta_{\epsilon_1}} (\epsilon_1 - \bar{\epsilon}) H(\bar{\epsilon} - \epsilon_1) \Big|_{\bar{\epsilon}_1 - \Delta_{\epsilon_1}}^{\bar{\epsilon}_1 + \Delta_{\epsilon_1}} \\ &= \frac{1}{2\Delta_{\epsilon_1}} [(\bar{\epsilon}_1 + \Delta_{\epsilon_1} - \bar{\epsilon}) H(\bar{\epsilon} - \bar{\epsilon}_1 - \Delta_{\epsilon_1}) - (\bar{\epsilon}_1 - \Delta_{\epsilon_1} - \bar{\epsilon}) H(\bar{\epsilon} - \bar{\epsilon}_1 + \Delta_{\epsilon_1})], \end{aligned} \tag{46}$$

$$\int_{\epsilon_1} H(\epsilon_1 - \bar{\epsilon}) P_{\epsilon_1}(\epsilon_1) \mathrm{d}\epsilon_1 = \frac{1}{2\Delta_{\epsilon_1}} [(\bar{\epsilon}_1 + \Delta_{\epsilon_1} - \bar{\epsilon}) H(\bar{\epsilon}_1 + \Delta_{\epsilon_1} - \bar{\epsilon}) - (\bar{\epsilon}_1 - \Delta_{\epsilon_1} - \bar{\epsilon}) H(\bar{\epsilon}_1 - \Delta_{\epsilon_1} - \bar{\epsilon})] \tag{47}$$

and

$$\int_{\epsilon_2} H(\epsilon_2 - \bar{\epsilon}) P_{\epsilon_2}(\epsilon_2) \mathrm{d}\epsilon_2 = \frac{1}{2\Delta_{\epsilon_2}} [(\bar{\epsilon}_2 + \Delta_{\epsilon_2} - \bar{\epsilon}) H(\bar{\epsilon}_2 + \Delta_{\epsilon_2} - \bar{\epsilon}) - (\bar{\epsilon}_2 - \Delta_{\epsilon_2} - \bar{\epsilon}) H(\bar{\epsilon}_2 - \Delta_{\epsilon_2} - \bar{\epsilon})]. \tag{48}$$

For a cellular material characterized by random distributions, the effective geometric stiffness then is given by

$$\begin{aligned} \tilde{A}(\bar{\epsilon}) = {} & \frac{\overline{A}_0(\bar{\epsilon}_1 + \Delta_{\epsilon_1} - \bar{\epsilon})}{2\Delta_{\epsilon_1}} H(\bar{\epsilon} - \bar{\epsilon}_1 - \Delta_{\epsilon_1}) - \frac{\overline{A}_0(\bar{\epsilon}_1 - \Delta_{\epsilon_1} - \bar{\epsilon})}{2\Delta_{\epsilon_1}} H(\bar{\epsilon} - \bar{\epsilon}_1 + \Delta_{\epsilon_1}) \\ & + \frac{\overline{A}_1(\bar{\epsilon}_1 + \Delta_{\epsilon_1} - \bar{\epsilon})}{2\Delta_{\epsilon_1}} H(\bar{\epsilon}_1 + \Delta_{\epsilon_1} - \bar{\epsilon}) - \frac{\overline{A}_1(\bar{\epsilon}_1 - \Delta_{\epsilon_1} - \bar{\epsilon})}{2\Delta_{\epsilon_1}} H(\bar{\epsilon}_1 - \Delta_{\epsilon_1} - \bar{\epsilon}) \\ & + \frac{(1 - \overline{A}_1)(\bar{\epsilon}_2 + \Delta_{\epsilon_2} - \bar{\epsilon})}{2\Delta_{\epsilon_2}} H(\bar{\epsilon}_2 + \Delta_{\epsilon_2} - \bar{\epsilon}) - \frac{(1 - \overline{A}_1)(\bar{\epsilon}_2 - \Delta_{\epsilon_2} - \bar{\epsilon})}{2\Delta_{\epsilon_2}} H(\bar{\epsilon}_2 - \Delta_{\epsilon_2} - \bar{\epsilon}), \end{aligned} \tag{49}$$

which can be represented in a slightly different, perhaps more transparent, form as

$$\tilde{A}(\overline{\epsilon}) = \begin{cases} \overline{A}_0, & \overline{\epsilon}_1 + \Delta_{\epsilon_1} \leqslant \overline{\epsilon} \leqslant 0, \\ \dfrac{(\overline{A}_0 - \overline{A}_1)\overline{\epsilon} - \overline{A}_0(\overline{\epsilon}_1 - \Delta_{\epsilon_1}) + \overline{A}_1(\overline{\epsilon}_1 + \Delta_{\epsilon_1})}{2\Delta_\epsilon}, & \overline{\epsilon}_1 - \Delta_{\epsilon_1} \leqslant \overline{\epsilon} \leqslant \overline{\epsilon}_1 + \Delta_{\epsilon_1}, \\ \overline{A}_1, & \overline{\epsilon}_2 + \Delta_{\epsilon_2} \leqslant \overline{\epsilon} \leqslant \overline{\epsilon}_1 - \Delta_{\epsilon_1}, \\ \dfrac{(\overline{A}_1 - 1)\overline{\epsilon} - \overline{A}_1(\overline{\epsilon}_2 - \Delta_{\epsilon_2}) + (\overline{\epsilon}_2 + \Delta_{\epsilon_2})}{2\Delta_{\epsilon_2}}, & \overline{\epsilon}_2 - \Delta_{\epsilon_2} \leqslant \overline{\epsilon} \leqslant \overline{\epsilon}_2 + \Delta_{\epsilon_2}, \\ 1, & -1 \leqslant \overline{\epsilon} \leqslant \overline{\epsilon}_2 - \Delta_{\epsilon_2}. \end{cases} \tag{50}$$

For a random distribution, the probability density function for the initial solid-volume fraction is given by

$$P_{\phi_0}(\phi_0) = \begin{cases} \dfrac{1}{2\Delta_\phi}, & \overline{\phi}_0 - \Delta_\phi \leqslant \phi_0 \leqslant \overline{\phi}_0 + \Delta_\phi \\ 0, & \text{otherwise} \end{cases} \tag{51}$$

in which $2\Delta_\phi$ is the range of permissible values of the initial solid-volume fraction, ϕ_0. Again, the quantity, Δ_ϕ, must be greater than zero, but must not be so large that the distribution becomes physically meaningless. For example, $\phi_0 \geqslant 0$, and thus $\overline{\phi}_0 - \Delta_\phi \geqslant 0$. This constraint ensures that the solid-volume fractions are physically realizable and provides lower and upper bounds on the permissible values of the initial solid-volume fraction for a particular foam cell, which in turn, provide lower and upper bounds on the average initial solid-volume fraction, and thus, on the average tangent modulus and the continuum-scale stress in the cellular material.

Upon substitution of the relation provided in Eq. (51), the integral in Eq. (35) is evaluated as

$$\int_{\phi_0} \phi_0^2 P_{\phi_0}(\phi_0)\mathrm{d}\phi_0 = \int_{\overline{\phi}_0 - \Delta_\phi}^{\overline{\phi}_0 + \Delta_\phi} \frac{\phi_0^2}{2\Delta_\phi}\mathrm{d}\phi_0 = \frac{3\overline{\phi}_0^2 + \Delta_\phi}{3}. \tag{52}$$

For a cellular material characterized by random distributions, the effective solid-volume fraction then is given by

$$\tilde{\phi}(\overline{\epsilon}) = \left[\frac{3\overline{\phi}_0^2 + \Delta_\phi}{3(1+\overline{\epsilon})}\right]^{\frac{1}{2}}. \tag{53}$$

Substitution of the relations provided in Eqs. (49) and (53) into the relation for the average tangent modulus provided in Eq. (33) yields a form of the average tangent modulus representing the collective mechanical response of a random dispersion of foam cells.

4.4. Gaussian distributions

Now, consider a cellular material, for which the parameters describing the cellular-scale mechanical response of any particular foam cell are characterized by Gaussian distributions. Many random variables studied in various physical experiments often have distributions that are approximately Gaussian. For example, a Gaussian distribution most often is a close approximation to the distribution of heights or weights of individuals taken at random from a homogeneous population of people, to the distribution of pore or crack sizes in samples of a particular metal, or to the distribution of tensile strengths for samples of a particular material. It is reasonable to expect that a Gaussian distribution is a close approximation to the distribution of parameters that describe the mechanical behavior of the cells taken at random from a sample of foam. In this case, the probability density functions for the transition strains are given by

$$P_{\epsilon_1}(\epsilon_1) = \frac{1}{\sqrt{2\pi}\sigma_{\epsilon_1}} \exp\left[\frac{-(\epsilon_1 - \overline{\epsilon}_1)^2}{2\sigma_{\epsilon_1}^2}\right] \tag{54}$$

and

$$P_{\epsilon_2}(\epsilon_2) = \frac{1}{\sqrt{2\pi}\sigma_{\epsilon_2}} \exp\left[\frac{-(\epsilon_2 - \overline{\epsilon}_2)^2}{2\sigma_{\epsilon_2}^2}\right] \tag{55}$$

in which σ_{ϵ_1} and σ_{ϵ_2} are the standard deviations in the distributions of ϵ_1 and ϵ_2, respectively, which provide measures of the dispersion of the distributions around the average values, $\overline{\epsilon}_1$ and $\overline{\epsilon}_2$. The standard deviations must be greater than zero, but must not be so large that the distributions become physically meaningless. For example, if $\overline{\epsilon}_1 + m\sigma_{\epsilon_1} \leqslant 0$ and $\overline{\epsilon}_2 - m\sigma_{\epsilon_2} \geqslant -1$, then by choosing an appropriate value for m, one can ensure that, to an acceptable probability, $-1 \leqslant \epsilon_1 \leqslant 0$ and $-1 \leqslant \epsilon_2 \leqslant 0$ (e.g., for $m = 1$, the probabilities that $\epsilon_1 \leqslant 0$ and $\epsilon_2 \geqslant -1$ are 0.842; for $m = 2$, the probabilities are 0.977; for $m = 3$, the probabilities are 0.999). Also, for the same reasons outlined above for random distributions, it is reasonable to assume that $\overline{\epsilon}_2 + m\sigma_{\epsilon_2} \leqslant \overline{\epsilon}_1 - m\sigma_{\epsilon_1}$. These constraints ensure that, to an acceptable probability, the transition strains are physically realizable and provide lower and upper bounds on the permissible values of the transition strains for a particular foam cell.

Upon substitution of the relations provided in Eqs. (54) and (55), the integrals in Eq. (34) are evaluated as

$$\begin{aligned}\int_{\epsilon_1} H(\overline{\epsilon} - \epsilon_1) P_{\epsilon_1}(\epsilon_1) \mathrm{d}\epsilon_1 &= \frac{1}{\sqrt{2\pi}\sigma_{\epsilon_1}} \int_{-\infty}^{0} H(\overline{\epsilon} - \epsilon_1) \exp\left[\frac{-(\epsilon_1 - \overline{\epsilon}_1)^2}{2\sigma_{\epsilon_1}^2}\right] \mathrm{d}\epsilon_1 \\ &\approx \frac{1}{\sqrt{2\pi}\sigma_{\epsilon_1}} \int_{-\infty}^{\infty} H(\overline{\epsilon} - \epsilon_1) \exp\left[\frac{-(\epsilon_1 - \overline{\epsilon}_1)^2}{2\sigma_{\epsilon_1}^2}\right] \mathrm{d}\epsilon_1 \\ &= \frac{1}{\sqrt{2\pi}\sigma_{\epsilon_1}} \int_{\overline{\epsilon}_1 - \overline{\epsilon}}^{\infty} \exp\left(\frac{-u^2}{2\sigma_{\epsilon_1}^2}\right) \mathrm{d}u = \frac{1}{2}\left[1 - \operatorname{erf}\left(\frac{\overline{\epsilon}_1 - \overline{\epsilon}}{\sqrt{2}\sigma_{\epsilon_1}}\right)\right],\end{aligned} \tag{56}$$

$$\int_{\epsilon_1} H(\epsilon_1 - \overline{\epsilon}) P_{\epsilon_1}(\epsilon_1) \mathrm{d}\epsilon_1 = \frac{1}{2}\left[1 - \operatorname{erf}\left(\frac{\overline{\epsilon} - \overline{\epsilon}_1}{\sqrt{2}\sigma_{\epsilon_1}}\right)\right] \tag{57}$$

and

$$\int_{\epsilon_2} H(\epsilon_2 - \overline{\epsilon}) P_{\epsilon_2}(\epsilon_2) \mathrm{d}\epsilon_2 = \frac{1}{2}\left[1 - \operatorname{erf}\left(\frac{\overline{\epsilon} - \overline{\epsilon}_2}{\sqrt{2}\sigma_{\epsilon_2}}\right)\right], \tag{58}$$

in which the function, $\operatorname{erf}(x)$, is the error function (or probability integral), defined by

$$\operatorname{erf}(x) \equiv \frac{2}{\sqrt{\pi}} \int_0^x \mathrm{e}^{-t^2} \mathrm{d}t. \tag{59}$$

For a cellular material characterized by Gaussian distributions, the effective geometric stiffness then is given by

$$\tilde{A}(\overline{\epsilon}) = \frac{\overline{A}_0}{2}\left[1 - \operatorname{erf}\left(\frac{\overline{\epsilon}_1 - \overline{\epsilon}}{\sqrt{2}\sigma_{\epsilon_1}}\right)\right] + \frac{\overline{A}_1}{2}\left[1 - \operatorname{erf}\left(\frac{\overline{\epsilon} - \overline{\epsilon}_1}{\sqrt{2}\sigma_{\epsilon_1}}\right)\right] + \frac{(1 - \overline{A}_1)}{2}\left[1 - \operatorname{erf}\left(\frac{\overline{\epsilon} - \overline{\epsilon}_2}{\sqrt{2}\sigma_{\epsilon_2}}\right)\right]. \tag{60}$$

For a Gaussian distribution, the probability density function for the initial solid-volume fraction is given by

$$P_{\phi_0}(\phi_0) = \frac{1}{\sqrt{2\pi}\sigma_\phi} \exp\left[\frac{-(\phi_0 - \overline{\phi}_0)^2}{2\sigma_\phi^2}\right], \tag{61}$$

in which σ_ϕ is the standard deviation in the distribution of ϕ_0, which provides a measure of the dispersion of the distribution around the average value, $\overline{\phi}_0$. Again, the standard deviation must be greater than zero, but must not be so large that the distribution becomes physically meaningless. For example, if $\overline{\phi}_0 - n\sigma_\phi \geqslant 0$, then by choosing an appropriate value for n, one can ensure that, to an acceptable probability, $\phi_0 \geqslant 0$. This constraint ensures that, to an acceptable probability, the solid-volume fractions are physically realizable and provides lower and upper bounds on the permissible values of the initial solid-volume fraction for a particular foam cell, which in turn, provide lower and upper bounds on the average initial solid-volume fraction, and thus, on the average tangent modulus and the continuum-scale stress in the cellular material.

Upon substitution of the relation provided in Eq. (61) the integral in Eq. (35) is evaluated as

$$\begin{aligned}\int_{\phi_0} \phi_0^2 P_{\phi_0}(\phi_0)\mathrm{d}\phi_0 &= \frac{1}{\sqrt{2\pi}\sigma_\phi}\int_0^\infty \phi_0^2 \mathrm{e}^{\frac{-(\phi_0-\overline{\phi}_0)^2}{2\sigma_\phi^2}}\mathrm{d}\phi_0 \approx \frac{1}{\sqrt{2\pi}\sigma_\phi}\int_{-\infty}^\infty \phi_0^2 \mathrm{e}^{\frac{-(\phi_0-\overline{\phi}_0)^2}{2\sigma_\phi^2}}\mathrm{d}\phi_0 \\ &= \frac{1}{\sqrt{2\pi}\sigma_\phi}\int_{-\infty}^\infty (u+\overline{\phi}_0)^2 \mathrm{e}^{\frac{-u^2}{2\sigma_\phi^2}}\mathrm{d}u = \overline{\phi}_0^2 + \sigma_\phi^2. \end{aligned} \tag{62}$$

For a cellular material characterized by Gaussian distributions, the effective solid-volume fraction then is given by

$$\tilde{\phi}(\overline{\epsilon}) = \left[\frac{\overline{\phi}_0^2 + \sigma_\phi^2}{(1+\overline{\epsilon})^2}\right]^{\frac{1}{2}}. \tag{63}$$

Substitution of the relations provided in Eqs. (60) and (63) into the relation for the average tangent modulus provided in Eq. (33) yields a form of the average tangent modulus representing the collective mechanical response of a disordered dispersion of foam cells characterized by Gaussian distributions.

4.5. Correlated variables

Despite the fact that the cellular-scale constitutive model is derived in such a way that the effects of the cellular-scale geometry, the properties of the parent solid, and the initial solid-volume fraction on the tangent modulus of the individual foam cell are uncorrelated, under certain circumstances, one might still expect some of independent variables to be correlated. For example, foam cells with a particular shape, or a particular orientation to loading, producing a stiffer-than-average initial response, are likely to exhibit a stiffer-than-average response for all levels of strain in that particular direction. In other words, for a particular cell, one might expect that

$$A_0 > \overline{A}_0 \Rightarrow A_1 > \overline{A}_1. \tag{64}$$

Also, as discussed in Section 2

$$\epsilon_2 \approx -1 + \phi_0. \tag{65}$$

In other words, one might expect the transition strain, ϵ_2, to be strongly correlated to the initial solid-volume fraction, ϕ_0.

Under these circumstances, with the Voigt approximation still in effect and with the initial tangent modulus of the parent solid remaining uncorrelated, the probability density function can be generalized to

$$P = P_1(A_0, A_1)P_{\epsilon_1}(\epsilon_1)P_2(\epsilon_2, \phi_0)P_{E^s}(E^s)\delta(\epsilon - \overline{\epsilon}), \tag{66}$$

in which $P_1(A_0, A_1)$ and $P_2(\epsilon_2, \phi_0)$ are joint or conditional probabilities. Substitution of the probability density function expressed in Eq. (66) into Eq. (29) provides a more general form of the average tangent modulus for correlated variables, which can be written as

$$\overline{E^{c}(\overline{\epsilon})} = \tilde{A}(\overline{\epsilon})\overline{E}^{s}[\tilde{\phi}(\overline{\epsilon})]^2 + (1-\overline{A}_1)\overline{E}^{s}[\tilde{\theta}(\overline{\epsilon})]^2 \tag{67}$$

in which

$$\tilde{A}(\overline{\epsilon}) = \overline{A}_0 \int_{\epsilon_1} H(\overline{\epsilon}-\epsilon_1)P_{\epsilon_1}(\epsilon_1)\mathrm{d}\epsilon_1 + \overline{A}_1 \int_{\epsilon_1} H(\epsilon_1-\overline{\epsilon})P_{\epsilon_1}(\epsilon_1)\mathrm{d}\epsilon_1, \tag{68}$$

$$\tilde{\phi}(\overline{\epsilon}) = \left[\frac{1}{(1+\overline{\epsilon})^2}\int_{\epsilon_2}\int_{\phi_0}\phi_0^2 P_2(\epsilon_2,\phi_0)\mathrm{d}\phi_0\mathrm{d}\epsilon_2\right]^{\frac{1}{2}} \tag{69}$$

and

$$\tilde{\theta}(\overline{\epsilon}) = \left[\frac{1}{(1+\overline{\epsilon})^2}\int_{\epsilon_2}\int_{\phi_0} H(\epsilon_2-\overline{\epsilon})\phi_0^2 P_2(\epsilon_2,\phi_0)\mathrm{d}\phi_0\mathrm{d}\epsilon_2\right]^{\frac{1}{2}}. \tag{70}$$

Note that, similar to the circumstances for which the independent variables are uncorrelated, the average tangent modulus only depends on the average values, $\overline{A}_0$, $\overline{A}_1$, and $\overline{E}^{s}$, rather than on the distributions of A_0, A_1, and E^{s}. It remains then to evaluate the integrals in Eqs. (68)–(70), which now depend on the joint probability, $P_2(\epsilon_2, \phi_0)$. In general, if a joint probability cannot be established through derivation, one must resort to direct numerical simulation to determine the corresponding probability density function.

For the remainder of this discussion, attention is restricted to the circumstances for which the independent variables are assumed to be uncorrelated. In Section 5, the various stochastic material representations presented in this section are combined with the continuum-scale constitutive model to obtain the stress–strain response for a cellular material subjected to finite-strain uni-axial compression.

5. Results and discussion

In this section, the stochastic constitutive model developed in Sections 2–4 is used to simulate the finite-strain uni-axial compression of disordered cellular materials to quasi-static loading conditions. The results are compared to previous modeling efforts and to experimental data obtained from tests on a commercially available, low-density, open-cell, polyurethane foam. Effects of varying material parameters and stochastic material representations also are examined. The material of interest represents one of the lightest of the structural foams, and is used extensively in cushioning, padding, and packaging applications.

A scanning electron micrograph of a polyurethane foam is shown in Fig. 1 (see Section 2). The parent solid (i.e., bulk polyurethane in the unfoamed state) has an average initial tangent modulus, $\overline{E}^{s} = 4.5 \times 10^4$ kPa. The effects of the foaming process on the properties of the parent solid are not understood well and provide a research topic of their own. Therefore, for present purposes, the properties of foamed and unfoamed polyurethane are assumed to be identical, spatially uniform, and independent of strain. Solid polyurethane has an average density, $\overline{\rho}^{s} = 1.2$ g/cm^3, while the average initial foam density was measured to be $\overline{\rho}_0^{c} = 0.036$ g/cm^3. Thus, this particular material has an average initial relative density, or average initial solid-volume fraction, $\overline{\phi}_0 = \overline{\rho}_0^{c}/\overline{\rho}^{s} = 0.03$. In other words, this material initially is 97% air by volume, and thus, typical of this class of materials, is very lightweight and very soft relative to the parent solid.

The continuum-scale stress–strain response of a polyurethane foam subjected to uni-axial compression is shown in Fig. 3. Experimental results are plotted as solid data points and are shown for three different foam samples, each nominally possessing the same average material properties.

Many models exist for predicting the initial properties of cellular materials, however, the classic analytic model developed by Gibson and Ashby (1988) also incorporates a buckling analysis to predict the level of stress for the "load plateau" and a model for densificatin to cover a full range of compressive strain. Results obtained using the Gibson and Ashby model are shown in Fig. 3 for purposes of comparison, and are plotted as a thin dotted line with open data points. For this model, the geometric constant of proportionality is set equal to unity, as suggested by the authors (see Gibson and Ashby, 1988, p.130).

Now, consider a monodisperse representation for the cellular material and the corresponding relation for the average tangent modulus given by Eq. (43). If $\overline{A}_1 = 0$ and if the nonlinear effects of strain on the solid-volume fraction are neglected (i.e., if $\tilde{\phi} = \overline{\phi}_0$), the average tangent modulus becomes

$$\overline{E}^{c} = [\overline{A}_0 H(\overline{\epsilon} - \overline{\epsilon}_1) + H(\overline{\epsilon}_2 - \overline{\epsilon})]\overline{E}^{s}\overline{\phi}_0^2. \tag{71}$$

This is equivalent to the model developed by Gibson and Ashby, provided that the material constants are chosen appropriately. (Because the experimental data only is available for $|\,\overline{\epsilon}\,| \leqslant 0.70$, the response corresponding to full densification is not shown in these figures.) Results obtained using the stochastic constitutive model for $\overline{A}_0 = 1$, $\overline{A}_1 = 0$, $\overline{\epsilon}_1 = -0.05$, $\overline{\epsilon}_2 = -0.97$, and $\tilde{\phi} = \overline{\phi}_0 = 0.03$ are plotted as the first dashed

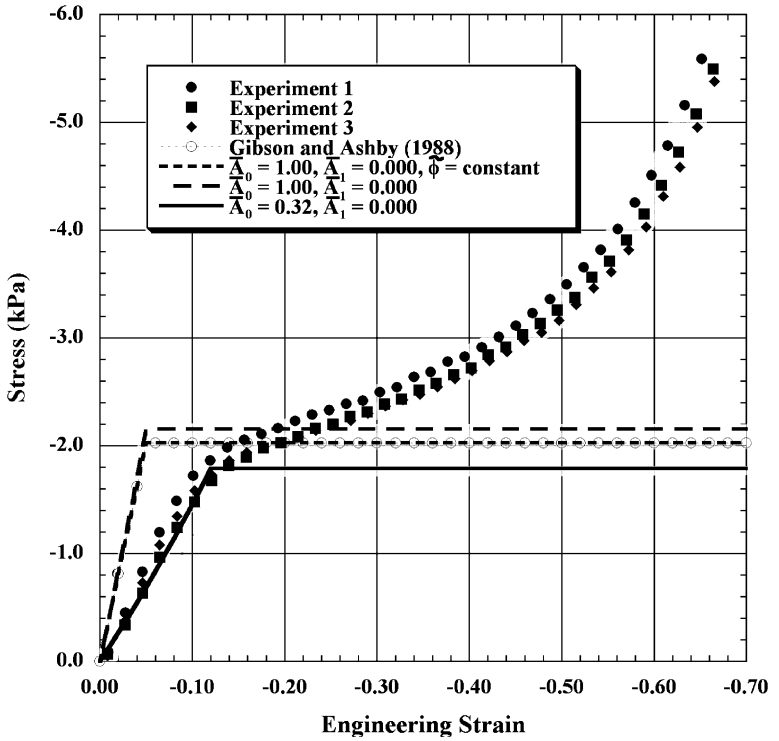

Fig. 3. The continuum-scale stress–strain response of a polyurethane foam subjected to quasi-static uni-axial compression. Experimental results are plotted as solid data points, the analytic model of Gibson and Ashby (1988) is plotted as a thin dashed line with open data points, and results obtained using the stochastic constitutive model with a monodisperse stochastic material representation are plotted as lines. The experimental data was provided courtesy of Dr. C. Liu of the Materials Science & Technology Division (MST-8) at Los Alamos National Laboratory.

line in Fig. 3. As expected, these results exactly reproduce the stress–strain response obtained using the Gibson and Ashby model. Results obtained for the same average material parameters, but with $\tilde{\phi} = \overline{\phi}_0/(1+\overline{\epsilon})$, are plotted as the second dashed line. The nonlinear effects associated with an evolving solid-volume fraction produce a slightly stiffer stress–strain response prior to the load plateau, which also is elevated to a higher level of stress.

The results presented in Fig. 3 show that the experimental stress–strain response is not reproduced accurately if $\overline{A}_0 = 1.0$ and $\overline{\epsilon}_1 = -0.05$. Experimental data for this material suggest that $0.30 \leqslant \overline{A}_0 \leqslant 0.35$ and $-0.16 \leqslant \overline{\epsilon}_1 \leqslant -0.08$. Results obtained using the stochastic constitutive model for $\overline{A}_0 = 0.32$, $\overline{A}_1 = 0$, $\overline{\epsilon}_1 = -0.12$, $\overline{\epsilon}_2 = -0.97$, and $\tilde{\phi} = \overline{\phi}_0/(1+\overline{\epsilon})$ are plotted in Fig. 3 as a solid line. This value of $\overline{A}_0$ produces a stress–strain response that more closely matches the experimental data prior to the onset of softening. While reproducing the initial stress–strain response, however, it remains clear that, for disordered foams like this polyurethane material, the idealization of a constant-stress load plateau is not very close to reality.

Results obtained using the stochastic constitutive model with a monodisperse representation and $\overline{A}_1 \neq 0$ are shown in Fig. 4. Here, the effects of varying the average geometric stiffness parameters, $\overline{A}_0$ and $\overline{A}_1$, on the continuum-scale stress–strain response are investigated. Again, the experimental results are plotted as solid data points, while the results obtained using the stochastic constitutive model are plotted as lines. Results are shown for $\overline{A}_0 = 0.26$ and $\overline{A}_1 = 0.031$, $\overline{A}_0 = 0.29$ and $\overline{A}_1 = 0.038$, $\overline{A}_0 = 0.32$ and $\overline{A}_1 = 0.045$, $\overline{A}_0 = 0.35$ and $\overline{A}_1 = 0.052$, and $\overline{A}_0 = 0.38$ and $\overline{A}_1 = 0.059$. The results obtained for $\overline{A}_0 = 0.32$ and $\overline{A}_1 = 0.045$ reproduce the experimental stress–strain response surprising well, however, one of the disadvan-

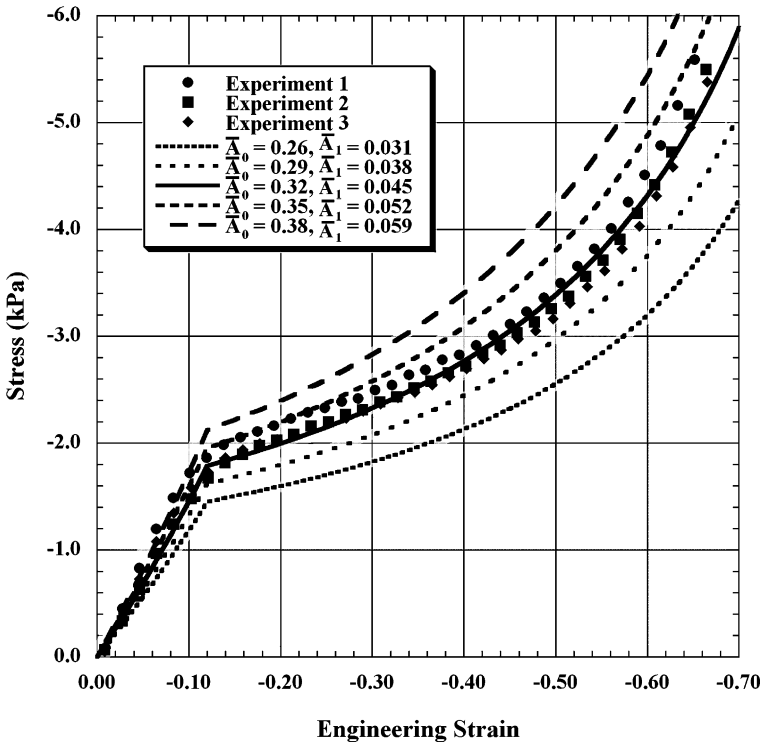

Fig. 4. The effects of varying average geometric stiffness parameters on the continuum-scale stress–strain response. Experimental results are plotted as solid data points, and results obtained using the stochastic constitutive model with a monodisperse stochastic material representation are plotted as lines.

tages associated with using monodisperse distributions becomes evident when one notices the discontinuous slope produced by the tri-linear approximation to the geometric stiffness. A smooth stress–strain response is produced when consideration is given to more realistic polydisperse distributions for the transition strains, ϵ_1 and ϵ_2.

Results obtained using random distributions for ϵ_1 and ϵ_2 are shown in Fig. 5. Here, the effects of introducing varying degrees of polydispersity into the distribution for ϵ_1 on the continuum-scale stress–strain response are investigated. For each calculation, $\overline{A}_0 = 0.32$, $\overline{A}_1 = 0.045$, $\overline{\epsilon}_1 = -0.12$, and $\overline{\epsilon}_2 = -0.97$, and results are plotted for $\Delta_{\epsilon_1} = 0.000$, 0.040, 0.080, and 0.120. Because the effects of polydispersity in the distribution for ϵ_2 are not realized at these levels of strain—even for the largest permissible values of Δ_{ϵ_2}—results are plotted only for $\Delta_{\epsilon_2} = 0.020$. The distribution for the initial solid-volume fraction remained monodisperse for these calculations. The results obtained for $\Delta_{\epsilon_1} = 0.000$ reproduce the stress–strain response obtained using a monodisperse distribution for ϵ_1, as expected. As the range of ϵ_1 increases, however, the average tangent modulus decreases for low-to-moderate strain, as some cells soften prior to reaching deformations corresponding to $\overline{\epsilon}_1$. And although the stress at moderate strain is affected slightly, the average tangent modulus in this regime of behavior remains unaffected.

Results obtained using random distributions for ϕ_0 are shown in Fig. 6. Here, the effects of introducing varying degrees of polydispersity into the distribution for ϕ_0 on the continuum-scale stress–strain response are investigated. For each calculation, $\overline{A}_0 = 0.32$, $\overline{A}_1 = 0.045$, $\overline{\epsilon}_1 = -0.12$, and $\overline{\epsilon}_2 = -0.97$, and results are plotted for $\Delta_\phi = 0.000$, 0.010, 0.020, and 0.030. The distributions for the transition strains remained monodisperse for these calculations. Again, the results obtained for $\Delta_\phi = 0.000$ reproduce the stress–strain

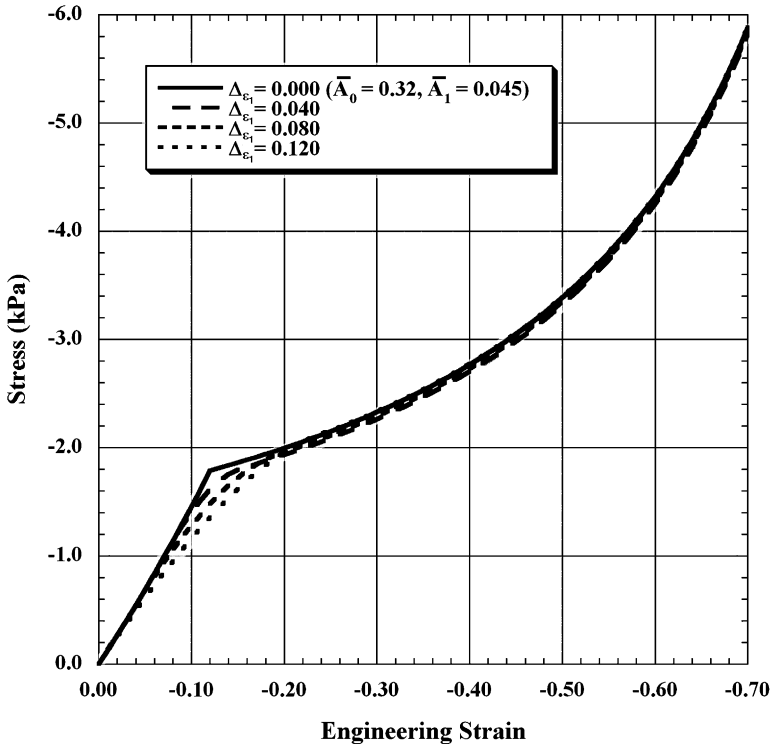

Fig. 5. The effects of varying random distributions for the transition strain, ϵ_1, on the continuum-scale stress–strain response. Results obtained for a monodisperse distribution are plotted as a solid line, while the results obtained for different ranges of ϵ_1 are plotted as dashed lines.

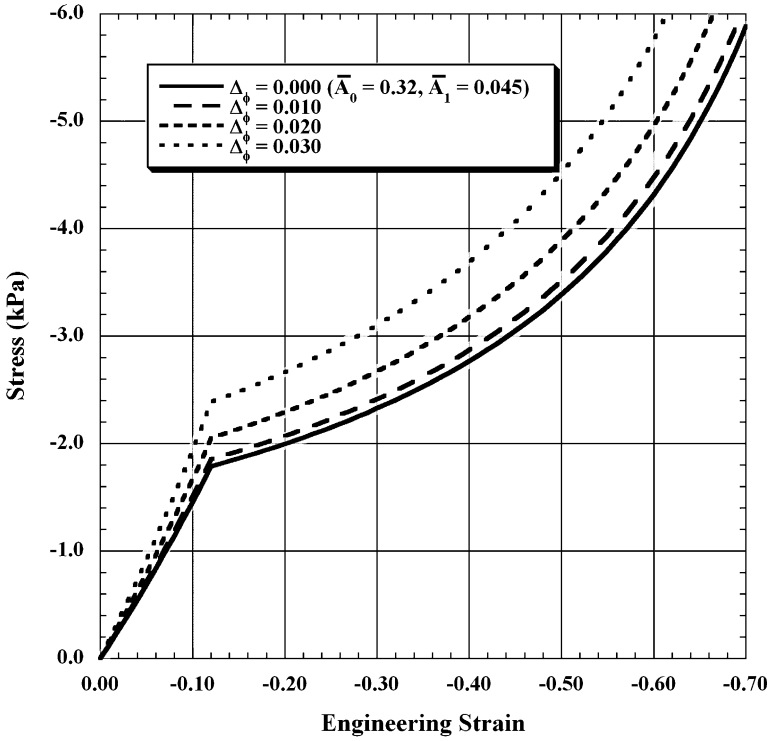

Fig. 6. The effects of varying random distributions for the initial solid-volume fraction, ϕ_0, on the continuum-scale stress–strain response. Results obtained for a monodisperse distribution are plotted as a solid line, while the results obtained for different ranges of ϕ_0 are plotted as dashed lines. For the given initial density, a cellular material with a wider dispersion of initial solid-volume fractions possesses a higher stiffness than one with a more narrow dispersion, suggesting that increasing degrees of polydispersity in the distribution of ϕ_0 produce an increasingly stiffer cellular material.

response obtained using a monodisperse distribution for ϕ_0, as expected. As the range of ϕ_0 increases, however, the average tangent modulus increases for all levels of strain. This is not intuitive, as the average initial solid-volume fraction, $\overline{\phi}_0$, remains constant. These results suggest that increasing degrees of polydispersity in the distribution of ϕ_0 produce an increasingly stiffer cellular material, and thus, extend the conclusions made by Van Der Burg et al. (1997) to finite-strain regimes of behavior.

Results obtained using Gaussian distributions for ϵ_1 are shown in Fig. 7. Again, the effects of introducing varying degrees of polydispersity into the distribution for ϵ_1 on the continuum-scale stress–strain response are investigated. For each calculation, $\overline{A}_0 = 0.32$, $\overline{A}_1 = 0.045$, $\overline{\epsilon}_1 = -0.12$, and $\overline{\epsilon}_2 = -0.97$, and results are plotted for $\sigma_{\epsilon_1} = 0.000$, 0.020, 0.040, and 0.060. For the reasons mentioned above, results are plotted only for $\sigma_{\epsilon_2} = 0.010$, and once again, the distribution for the initial solid-volume fraction remained monodisperse for these calculations. The results obtained for $\sigma_{\epsilon_1} = 0.000$ reproduce the stress–strain response obtained using a monodisperse distribution for ϵ_1, as expected. As the standard deviation increases, however, the average tangent modulus decreases for low-to-moderate strain, as some cells soften prior to reaching deformations corresponding to $\overline{\epsilon}_1$. And although the stress at moderate strain is affected slightly, the average tangent modulus in this regime of behavior remains unaffected.

Results obtained using Gaussian distributions for ϕ_0 are shown in Fig. 8. Again, the effects of introducing varying degrees of polydispersity into the distribution for ϕ_0 on the continuum-scale stress–strain response are investigated. For each calculation, $\overline{A}_0 = 0.32$, $\overline{A}_1 = 0.045$, $\overline{\epsilon}_1 = -0.12$, and $\overline{\epsilon}_2 = -0.97$, and

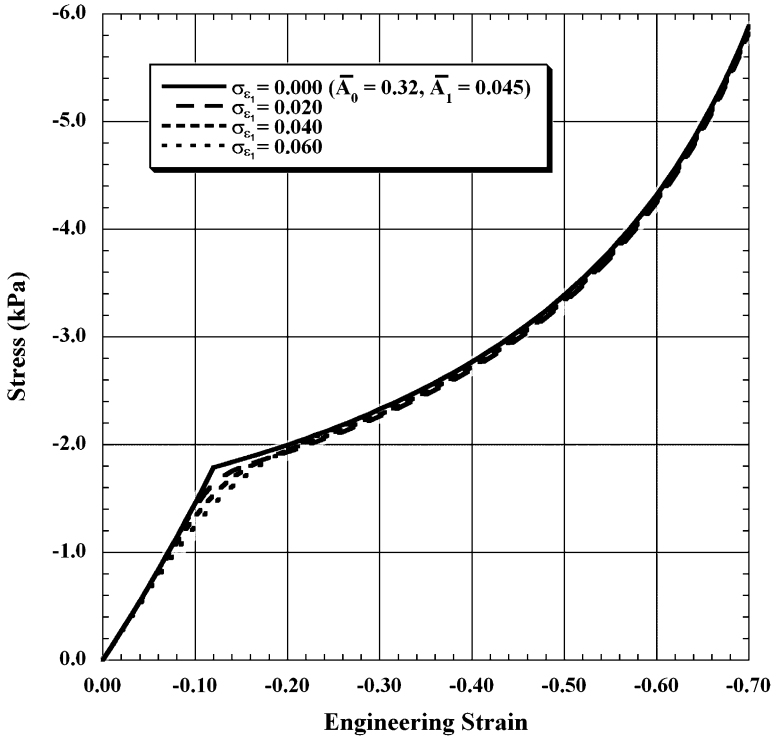

Fig. 7. The effects of varying Gaussian distributions for the transition strain, ϵ_1, on the continuum-scale stress–strain response. Results obtained for a monodisperse distribution are plotted as a solid line, while the results obtained for different standard deviations in the distribution of ϵ_1 are plotted as dashed lines.

results are plotted for $\sigma_\phi = 0.000$, 0.005, 0.010, and 0.015. The distributions for the transition strains remained monodisperse for these calculations. Again, the results obtained for $\sigma_\phi = 0.000$ reproduce the stress–strain response obtained using a monodisperse distribution for ϕ_0, as expected. As the standard deviation increases, however, the average tangent modulus increases for all levels of strain. Once again, despite the fact that the average initial solid-volume fraction, $\overline{\phi}_0$, remains constant, increasing degrees of polydispersity in the distribution of ϕ_0 produce an increasingly stiffer cellular material.

Results obtained using the stochastic constitutive model and Gaussian distributions for ϵ_1, ϵ_2, and ϕ_0 are shown in Fig. 9. For each calculation, $\overline{A}_0 = 0.32$, $\overline{A}_1 = 0.038$, $\overline{\epsilon}_1 = -0.12$, and $\overline{\epsilon}_2 = -0.97$, however, the calculated stress–strain response obtained using four different stochastic material representations are shown. Results are plotted for $\sigma_{\epsilon_1} = 0.060$ and $\sigma_\phi = 0.000$, $\sigma_{\epsilon_1} = 0.040$ and $\sigma_\phi = 0.005$, $\sigma_{\epsilon_1} = 0.020$ and $\sigma_\phi = 0.010$, and $\sigma_{\epsilon_1} = 0.000$ and $\sigma_\phi = 0.015$. Again, for the reasons mentioned above, results are plotted only for $\sigma_{\epsilon_2} = 0.010$. The results obtained for $\sigma_{\epsilon_1} = 0.060$ and $\sigma_\phi = 0.000$, and for $\sigma_{\epsilon_1} = 0.000$ and $\sigma_\phi = 0.015$, represent lower and upper bounds, respectively, on the stress–strain response for this particular set of average material parameters. The experimental results also are shown in Fig. 9 and one can see that the data is contained within these bounds. Also, one can see that the results obtained for $\sigma_{\epsilon_1} = 0.020$ and $\sigma_\phi = 0.010$ reproduce the experimental stress–strain response quite well.

Results obtained using Gaussian distributions for ϵ_1, ϵ_2, and ϕ_0 also are shown in Fig. 10. For each calculation, $\overline{A}_0 = 0.32$, $\overline{A}_1 = 0.038$, $\overline{\epsilon}_1 = -0.12$, $\sigma_{\epsilon_1} = 0.020$, $\overline{\epsilon}_2 = -0.97$, and $\sigma_{\epsilon_2} = 0.010$. The stress–strain response obtained for $\overline{\phi}_0 = 0.0300$ using three different distributions for ϕ_0 are shown and compared with results obtained using monodisperse distributions for ϕ_0 and three different values of the average initial

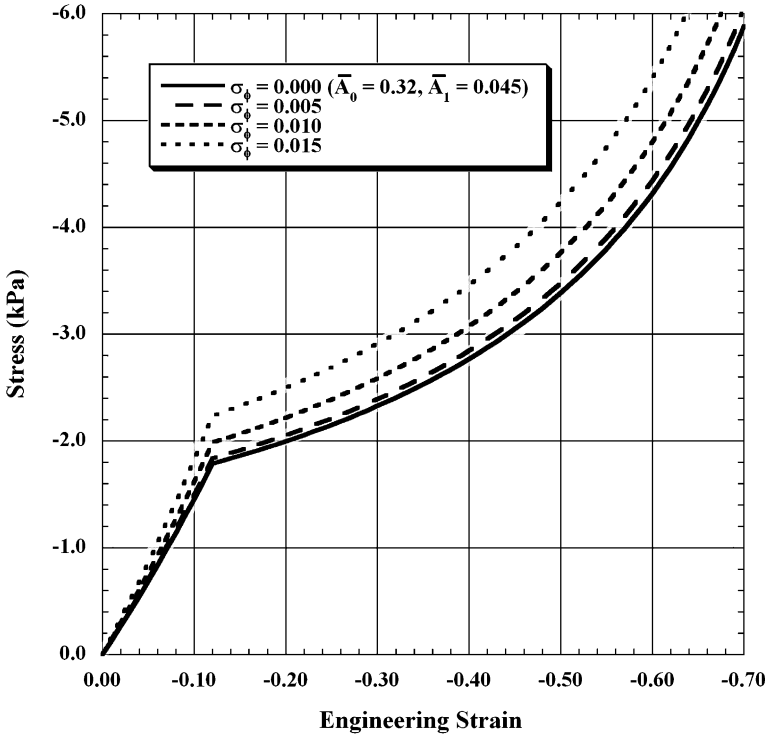

Fig. 8. The effects of varying Gaussian distributions for the initial solid-volume fraction, ϕ_0, on the continuum-scale stress–strain response. Results obtained for a monodisperse distribution are plotted as a solid line, while the results obtained for different standard deviations in the distribution of ϕ_0 are plotted as dashed lines.

solid-volume fraction, $\overline{\phi}_0$. Results for $\overline{\phi}_0 = 0.0300$ and $\sigma_\phi = 0.000$, $\overline{\phi}_0 = 0.0300$ and $\sigma_\phi = 0.005$, $\overline{\phi}_0 = 0.0300$ and $\sigma_\phi = 0.010$, and $\overline{\phi}_0 = 0.0300$ and $\sigma_\phi = 0.015$ are plotted as thin solid lines with open data points. Results for $\overline{\phi}_0 = 0.0304$ and $\sigma_\phi = 0.000$, $\overline{\phi}_0 = 0.0316$ and $\sigma_\phi = 0.000$, and $\overline{\phi}_0 = 0.0335$ and $\sigma_\phi = 0.000$ are plotted as dashed lines. The results show that for a given initial density, a cellular material with a wider dispersion of cells possesses a higher stiffness than one with a more narrow dispersion and that the effects of increasing the degree of polydispersity produces the same stiffening effects as increasing the initial solid-volume fraction.

6. Concluding remarks

It has been long recognized that the characteristic, nonlinear, mechanical response exhibited by cellular materials at the continuum scale is inherently related to the intricate structure and the physical mechanisms of deformation occuring at the length scale associated with an individual foam cell. Previous efforts to model the macroscopic mechanical response of cellular materials, therefore, have focused attention on simplified mechanical descriptions of single, idealized, foam cells or suitable representative structures. The advantage of using a single-cell approach to model the response of cellular materials lies in the fact that the simple mechanical descriptions provide the most tractable means of incorporating cellular-scale deformation mechanisms into a continuum-scale response model. Such efforts lead to more physically based modeling capabilities than can be achieved through purely phenomenological or numerical modeling approaches.

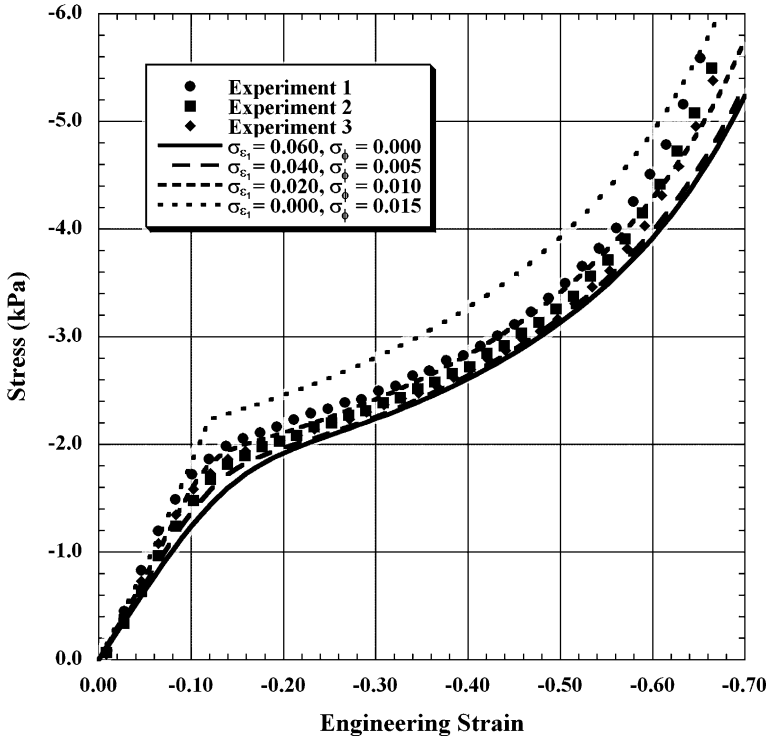

Fig. 9. The continuum-scale stress–strain response of a polyurethane foam subjected to quasi-static uni-axial compression. Experimental results are plotted as solid data points, while the results obtained for different Gaussian distributions are plotted as lines. Particular stochastic material representations provide upper and lower bounds on the stress–strain response, while a suitable choice for the stochastic representation reproduces the experimental stress–strain data quite well.

The single-cell view alone, however, oversimplifies the actual physical response taking place in the underlying structures as cellular materials deform. Most often, the single-cell approach has been used to calculate initial, linearly elastic properties of cellular materials, but rarely to generate a description of the evolving nonlinear properties. Previous modeling efforts largely have ignored the disordered nature of the underlying cellular structure. Many of the models that have been developed have been formulated on the basis of an assumed structural uniformity that does not exist in materials with disordered structure, and such models have come to rely on nonphysical mechanisms at the cellular scale, such as buckling, to describe certain features in the material response at the continuum scale. Most importantly, a physically based constitutive model that is valid through the large deformations for which these materials are intended previously has not been forthcoming.

In the present work, the development of a continuum-scale constitutive model begins with a cellular-scale mechanical response description generalized to accommodate finite strain. As in previous studies, the mechanical model used is based on cellular-scale deformation mechanisms. But unlike in previous studies, the nonlinear response associated with large deformations is considered. The cellular-scale mechanical model then is averaged over an ensemble of foam cells, forming a continuum-scale constitutive model that relates the macroscopic stress rate in the cellular material to the macroscopic strain rate. Various stochastic material representations are considered through the use of probability density functions for the relevant material parameters, and closure models for the continuum-scale constitutive model are obtained.

The stochastic constitutive model is used to calculate the continuum-scale mechanical response of a low-density, open-cell, polyurethane foam to finite-strain uni-axial compression. The stress–strain response

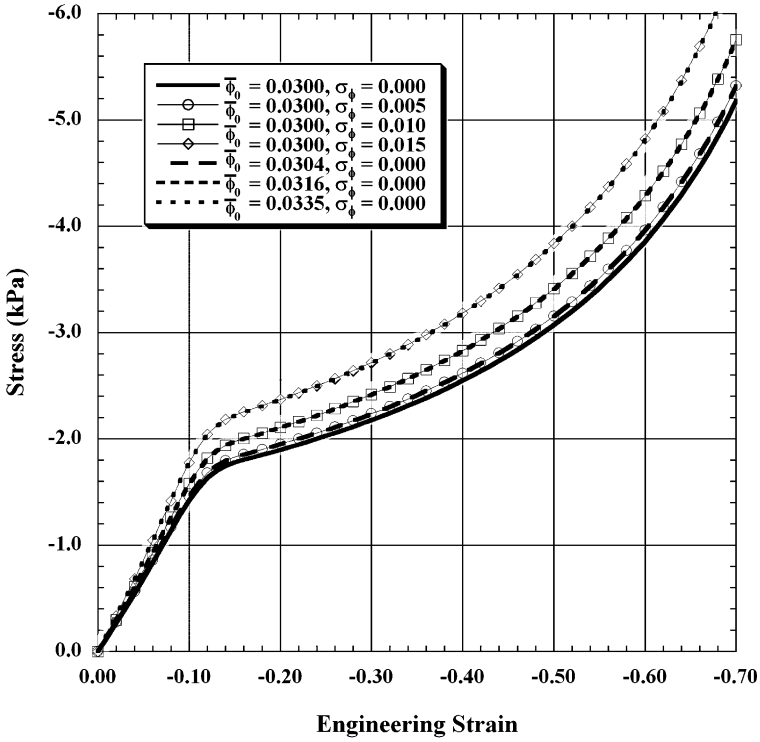

Fig. 10. The corresponding effects of increasing degrees of polydispersity and increasing average initial solid-volume fraction on the continuum-scale stress–strain response. Results obtained for a monodisperse distribution are plotted as a solid line, the results obtained for $\overline{\phi}_0 = 0.0300$ and different standard deviations in the distribution of ϕ_0 are plotted as thin solid lines with open data points, and the results obtained for $\sigma_\phi = 0.000$ and different values of the average initial solid-volume fraction are plotted as dashed lines. The results show that the effects of increasing the degree of polydispersity produces the same stiffening effects as increasing the initial solid-volume fraction.

obtained using the stochastic constitutive model is compared to experimental data, and the effects of various stochastic material representations on the macroscopic behavior are studied. Results demonstrate that for a given initial density, a cellular material with a wider dispersion of cells can possess a higher stiffness than one with a more narrow dispersion and that increasing the material's degree of polydispersity can produce the same stiffening effects as increasing the initial solid-volume fraction. Additionally, particular stochastic representations are shown to provide upper and lower bounds on the stress–strain response of the cellular material under investigation, while suitable choices for the stochastic representation are shown to accurately reproduce the stress–strain response through the large deformations associated with densification, where most other models and direct numerical simulations fail.

The objective of this work is to develop a more physically based constitutive model, and thus a more predictive capability for simulating the mechanical response of disordered cellular materials. Coupling a nonlinear, cellular-scale, mechanical model with a stochastic material representation provides a more realistic depiction of the response of these highly disordered materials and affords the opportunity to study these materials through the large deformations for which they are designed. The stochastic approach, furthermore, allows one to investigate the effects of variability in cellular-scale structure and properties on the continuum-scale response of these materials.

Future research will focus on generalizing the model presented here to include a more complete physical description of the relevant cellular-scale deformation mechanisms. Specifically, in addition to the dominant

bending mechanisms already considered, axial, torsional, strain-softening, and contact mechanisms will be represented in the construction of the cellular-scale constitutive model. The mechanics of closed-cell foams also will be considered. Furthermore, appropriate numerical techniques will be pursued to investigate and quantify the true stochastic nature of the cellular-scale material parameters. A likely candidate in this regard is the Material Point Method discussed by Bardenhagen et al. (2004). In future work, the Voigt and Reuss approximations will be relaxed and models will be developed for the cross-correlation terms that appear in the expressions for the average rates of stress and strain. The constitutive model will be generalized to three dimensions and both path- and rate-dependent response will be considered. Additionally, a modeling approach suitable for describing the response of cellular materials to shock and other highly dynamic loading conditions will be pursued. Modeling the rate-dependent dynamic response of cellular materials requires a description for the coupled effects of the permeating fluid. Extensions of the constitutive model developed here for such situations are the subjects of several forthcoming articles.

Acknowledgements

This work was performed under the auspices of the U. S. Department of Energy, under contract W–7405–ENG–36 with the University of California. The authors would like to acknowledge helpful discussions with Drs. W.B. Van der Heyden, D.Z. Zhang, T.O. Williams, and R.M. Rauenzahn of the Theoretical Division's Fluid Dynamics Group (T-3) at Los Alamos National Laboratory.

References

Ashby, M.F., 1983. The mechanical properties of cellular solids. Metallurgical Transactions, A. Physical Metallurgy and Materials Science 14 (9), 1755–1769.

Bardenhagen, S.G., Brydon, A.D., Guilkey, J.E., 2004. Insight into the physics of foam densification via numerical simulation. Journal of the Mechanics and Physics of Solids 53 (3), 597–617.

Gent, A.N., Thomas, A.G., 1959a. The deformations of foamed elastic materials. Journal of Applied Polymer Science 1 (1), 107–113.

Gent, A.N., Thomas, A.G., 1959b. Failure of foamed elastic materials. Journal of Applied Polymer Science 2 (6), 354–357.

Gent, A.N., Thomas, A.G., 1963. Mechanics of foamed elastic materials. Rubber Chemistry and Technology 36 (3), 597–610.

Gibson, L.J., Ashby, M.F., 1982. The mechanics of three-dimensional cellular materials. Proceedings of the Royal Society of London, A: Mathematical and Physical Sciences 382 (1782), 43–59.

Gibson, L.J., Ashby, M.F., 1988. Cellular Solids: Structure and Properties. Pergamon Press, Oxford, UK.

Gibson, L.J., Ashby, M.F., Schajer, G.S., Robertson, C.I., 1982. The mechanics of two-dimensional cellular materials. Proceedings of the Royal Society of London, A: Mathematical and Physical Sciences 382 (1782), 25–42.

Hilyard, N.C. (Ed.), 1982. Mechanics of Cellular Plastics. Macmillan, New York.

Kraynik, A.M., Neilsen, M.K., Reinelt, D.A., Warren, W.E., 1999. Foam micromechanics: structure and rheology of foams, emulsions, and cellular solids. In: Sadoc, J.F., Rivier, N. (Eds.), Foams and Emulsions. Kluwer Academic Publishers, Amsterdam, The Netherlands.

Laroussi, M., Sab, K., Alaoui, A., 2002. Foam mechanics: nonlinear response of an elastic 3D-periodic microstructure. International Journal of Solids and Structures 39 (13–14), 3599–3623.

Reuss, A., 1929. Berechnung der Fliessgrenze von Mischkristallen auf Grund der Plastizitätsbedingung für Einkristalle. Zeitschrift für Angewandte der Mathematik und Mechanik 9 (1), 49–58.

Schjødt-Thomsen, J., Pyrz, R., 2004. Influence of statistical cell dispersion on the local strain and overall properties of cellular materials. American Institute of Physics Conference Proceedings 712 (1), 1630–1638.

Talalay, J.A., 1949. Load-carrying capacity of latex foam rubber. Industrial and Engineering Chemistry 46 (7), 1530–1538.

Triantafyllidis, N., Schraad, M.W., 1998. Onset of failure in aluminum honeycombs under general in-plane loading. Journal of the Mechanics and Physics of Solids 46 (6), 1089–1124.

Van Der Burg, M.W.D., Shulmeister, V., Van Der Geissen, E., Marissen, R., 1997. On the linear elastic properties of regular and random open-cell foam models. Journal of Cellular Plastics 33 (1), 31–54.

Voigt, W., 1889. Ueber die Beziehung zwischen den beiden Elasticitätsconstanten isotroper Körper. Annalen der Physik und Chemie 38 (12), 573–587.

Warren, W.E., Kraynik, A.M., 1987. Foam mechanics: the linear elastic response of two-dimensional spatially periodic cellular materials. Mechanics of Materials 6 (1), 27–37.

Warren, W.E., Kraynik, A.M., 1988. The linear elastic properties of open-cell foams. Journal of Applied Mechanics 55 (2), 341–346.

Warren, W.E., Kraynik, A.M., Stone, C.M., 1989. A constitutive model for two-dimensional nonlinear elastic foams. Journal of the Mechanics and Physics of Solids 37 (6), 717–733.

Warren, W.E., Kraynik, A.M., 1991. The nonlinear elastic behavior of open-cell foams. Journal of Applied Mechanics 58 (2), 376–381.

Warren, W.E., Kraynik, A.M., 1997. Linear elastic behavior of a low-density Kelvin foam with open cells. Journal of Applied Mechanics 64 (4), 787–794.

Zhu, H.X., Mills, N.J., Knott, J.F., 1997. Analysis of the high strain compression of open-cell foams. Journal of the Mechanics and Physics of Solids 45 (11–12), 1875–1904.

Zhu, H.X., Hobdell, J.R., Windle, A.H., 2000. Effects of cell irregularity on the elastic properties of open-cell foams. Acta Materialia 48 (20), 4893–4900.

Zhu, H.X., Windle, A.H., 2002. Effects of cell irregularity on the high strain compression of open-cell foams. Acta Materialia 50 (5), 1041–1052.